

## Controlled human malaria infection with a clone of *Plasmodium vivax* with high quality genome assembly

Angela M. Minassian, ... , Julian C. Rayner, Simon J. Draper

JCI Insight. 2021. <https://doi.org/10.1172/jci.insight.152465>.

Resource and Technical Advance In-Press Preview Infectious disease

Controlled human malaria infection (CHMI) provides a highly informative means to investigate host-pathogen interactions and enable in vivo proof-of-concept efficacy testing of new drugs and vaccines. However, unlike *Plasmodium falciparum*, well-characterized *P. vivax* parasites that are safe and suitable for use in modern CHMI models are limited. Here, two healthy malaria-naïve UK adults with universal donor blood group were safely infected with a clone of *P. vivax* from Thailand by mosquito-bite CHMI. Parasitemia developed in both volunteers and, prior to treatment, each volunteer donated blood to produce a cryopreserved stabilate of infected red blood cells. Following stringent safety screening, the parasite stabilate from one of these donors (“PvW1”) was thawed and used to inoculate six healthy malaria-naïve UK adults by blood-stage CHMI, at three different dilutions. Parasitemia developed in all volunteers, who were then successfully drug treated. PvW1 parasite DNA was isolated and sequenced to produce a high quality genome assembly by using a hybrid assembly method. We analysed leading vaccine candidate antigens and multigene families, including the Vivax interspersed repeat (VIR) genes of which we identified 1145 in the PvW1 genome. Our genomic analysis will guide future assessment of candidate vaccines and drugs, as well as experimental medicine studies.

Find the latest version:

<https://jci.me/152465/pdf>



1 **Controlled human malaria infection with a clone of**  
2 ***Plasmodium vivax* with high quality genome assembly**

3  
4 Angela M. Minassian<sup>1\*</sup>, Yrene Themistocleous<sup>1†</sup>, Sarah E. Silk<sup>1,2</sup>, Jordan R. Barrett<sup>1,2</sup>, Alison Kemp<sup>3,4</sup>,  
5 Doris Quinkert<sup>1,2</sup>, Carolyn M. Nielsen<sup>1,2</sup>, Nick J. Edwards<sup>1</sup>, Thomas A. Rawlinson<sup>1</sup>, Fernando Ramos  
6 Lopez<sup>1</sup>, Wanlapa Roobsoong<sup>5</sup>, Katherine J. Ellis<sup>1</sup>, Jee-Sun Cho<sup>1</sup>, Eerik Aunin<sup>3</sup>, Thomas D. Otto<sup>3</sup>, Adam J.  
7 Reid<sup>3</sup>, Florian Bach<sup>6</sup>, Geneviève M. Labbé<sup>1</sup>, Ian D. Poulton<sup>1</sup>, Arianna Marini<sup>1</sup>, Marija Zaric<sup>1</sup>, Margaux  
8 Mulatier<sup>1</sup>, Raquel Lopez Ramon<sup>1</sup>, Megan Baker<sup>1</sup>, Celia H. Mitton<sup>1</sup>, Jason C. Sousa<sup>7</sup>, Nattawan  
9 Rachaphaew<sup>5</sup>, Chalermpon Kumpitak<sup>5</sup>, Nongnuj Maneechai<sup>5</sup>, Chayanut Suansomjit<sup>5</sup>, Tianrat Piteekan<sup>8</sup>,  
10 Mimi M. Hou<sup>1</sup>, Baktash Khozoe<sup>1</sup>, Kirsty McHugh<sup>1,2</sup>, David J. Roberts<sup>9</sup>, Alison M. Lawrie<sup>1</sup>, Andrew M.  
11 Blagborough<sup>10</sup>, Fay L. Nugent<sup>1</sup>, Iona J. Taylor<sup>1</sup>, Kimberly J. Johnson<sup>1</sup>, Philip J. Spence<sup>6</sup>, Jetsumon  
12 Sattabongkot<sup>5</sup>, Sumi Biswas<sup>1</sup>, Julian C. Rayner<sup>3,4</sup>, and Simon J. Draper<sup>1,2\*</sup>.

13  
14 <sup>1</sup> The Jenner Institute, University of Oxford, Oxford, UK.

15 <sup>2</sup> Department of Biochemistry, University of Oxford, Oxford, UK.

16 <sup>3</sup> Wellcome Sanger Institute, Wellcome Genome Campus, Cambridge, UK.

17 <sup>4</sup> Cambridge Institute for Medical Research, University of Cambridge, Cambridge, UK.

18 <sup>5</sup> Mahidol Vivax Research Unit, Faculty of Tropical Medicine, Mahidol University, Bangkok 10400,  
19 Thailand.

20 <sup>6</sup> Institute of Immunology and Infection Research, University of Edinburgh, Edinburgh, UK.

21 <sup>7</sup> Walter Reed Army Institute of Research, 503 Robert Grant Avenue, Silver Spring, MD 20910, USA.

22 <sup>8</sup> Mahidol-Oxford Tropical Medicine Research Unit, Faculty of Tropical Medicine, Mahidol University,  
23 Bangkok 10400, Thailand.

24 <sup>9</sup> Nuffield Division of Clinical Laboratory Sciences, Radcliffe Department of Medicine, University of  
25 Oxford, Oxford, UK.

26 <sup>10</sup> Department of Pathology, University of Cambridge, Cambridge, UK.

27 <sup>†</sup> These authors contributed equally.

28 <sup>\*</sup> Corresponding authors: AMM ([angela.minassian@ndm.ox.ac.uk](mailto:angela.minassian@ndm.ox.ac.uk)): Centre for Clinical Vaccinology and  
29 Tropical Medicine, University of Oxford, Churchill Hospital, Oxford, OX3 7LA, United Kingdom; and SJD

30 ([simon.draper@bioch.ox.ac.uk](mailto:simon.draper@bioch.ox.ac.uk)): Department of Biochemistry, South Parks Road, Oxford, OX1 3QU,  
31 United Kingdom, Tel: +44-1865-285438.

32 **Abstract**

33 Controlled human malaria infection (CHMI) provides a highly informative means to investigate host-  
34 pathogen interactions and enable *in vivo* proof-of-concept efficacy testing of new drugs and vaccines.  
35 However, unlike *Plasmodium falciparum*, well-characterized *P. vivax* parasites that are safe and suitable  
36 for use in modern CHMI models are limited. Here, two healthy malaria-naïve UK adults with universal  
37 donor blood group were safely infected with a clone of *P. vivax* from Thailand by mosquito-bite CHMI.  
38 Parasitemia developed in both volunteers and, prior to treatment, each volunteer donated blood to  
39 produce a cryopreserved stabilate of infected red blood cells. Following stringent safety screening, the  
40 parasite stabilate from one of these donors (“PvW1”) was thawed and used to inoculate six healthy  
41 malaria-naïve UK adults by blood-stage CHMI, at three different dilutions. Parasitemia developed in all  
42 volunteers, who were then successfully drug treated. PvW1 parasite DNA was isolated and sequenced to  
43 produce a high quality genome assembly by using a hybrid assembly method. We analysed leading  
44 vaccine candidate antigens and multigene families, including the Vivax interspersed repeat (VIR) genes  
45 of which we identified 1145 in the PvW1 genome. Our genomic analysis will guide future assessment of  
46 candidate vaccines and drugs, as well as experimental medicine studies.

47

## 48 **Introduction**

49 The majority of human malaria is caused by two species of parasite – *Plasmodium falciparum* and *P.*  
50 *vivax*. Infection is initiated by an infected *Anopheles* mosquito bite, delivering sporozoites which rapidly  
51 migrate to and infect the liver. Asexual replication in the liver sees each infected cell produce thousands  
52 of merozoites. These rupture out into the blood and infect red blood cells (RBC), before undergoing  
53 exponential growth that leads to clinical symptoms and the associated morbidity and mortality. *P. vivax*  
54 is the predominant cause of malaria outside of Africa and is more geographically widespread than *P.*  
55 *falciparum*, with 2.5 billion people living at risk in Latin America, Oceania, Asia and the horn of Africa (1).  
56 Moreover, recent data demonstrate a significant burden of morbidity and associated mortality in young  
57 children and pregnant women (2), challenging the long-held dogma that this parasite is “benign” (3).

58 A number of factors also underlie the differing epidemiology of *P. vivax* and make it more difficult to  
59 control and eliminate than *P. falciparum* (4). Most notably earlier development of gametocytes leads to  
60 transmission prior to symptom onset, and its ability to form dormant liver-stage forms, termed  
61 “hypnozoites”, causes waves of relapsing blood-stage parasitemia and sustained transmission (5).  
62 However, despite a clear global health need to develop an effective vaccine and improved antimalarial  
63 drugs, these efforts continue to lag behind those for *P. falciparum*. The reasons for this are numerous,  
64 but perhaps most significant is the fact that *P. vivax* has not been able to be adapted to long-term *in*  
65 *vitro* culture, despite extensive efforts. This has severely limited laboratory studies, as well as the  
66 development of modern controlled human malaria infection (CHMI) models, which rely on a well-  
67 defined isolate of *P. vivax*, and would enable *in vivo* efficacy testing of candidate vaccines and anti-  
68 malarial drugs in proof-of-concept clinical trials. This is in contrast to *P. falciparum* where *in vitro* culture  
69 and sophisticated genetic modification experiments are carried out all over the world, and CHMI can be  
70 initiated by the traditional mosquito-bite method, or by injection of cryopreserved sporozoites or an  
71 inoculum of blood-stage parasites (6). Most of these studies have been carried out in non-endemic  
72 settings, but CHMI trial capacity is now expanding across endemic countries in Africa, enabled by the use  
73 of cryopreserved sporozoites. In contrast, modern CHMI with *P. vivax* has been less utilized, with only a  
74 handful of studies reported (7).

75 For mosquito-bite *P. vivax* CHMI trials, most have taken place in Cali, Columbia (8-11) plus one at the  
76 Walter Reed Army Institute of Research (WRAIR), USA (12), with 108 volunteers challenged in total. Such  
77 trials necessitate production of infected mosquitoes in an endemic setting using fresh gametocytes from  
78 an infected patient. Shipment of the mosquitoes to non-endemic areas, and timing these activities with

79 recruitment of volunteers who may receive an intervention such as a vaccine, poses significant logistical  
80 challenges. Moreover, a different isolate of *P. vivax* is inevitably used for every trial which can hamper  
81 interpretation of the results and inter-study comparability. These studies also pose the risk of relapse,  
82 and thus require participants to be screened for glucose-6-phosphate dehydrogenase (G6PD) deficiency  
83 (to avoid hemolysis induced by primaquine treatment). They also require assessment of the volunteers'  
84 ability to metabolize primaquine, given relapsing infection occurred in two volunteers in the CHMI study  
85 at WRAIR despite primaquine treatment. Here, drug failure was subsequently linked to the volunteers'  
86 cytochrome P450 2D6 (CYP2D6) genotypes that were predicted to be poor or intermediate metabolizer  
87 phenotypes of the drug (13).

88 The use of the blood-stage CHMI model (14, 15) has several advantages over mosquito-bite CHMI,  
89 although it does not mimic the route of natural infection. Here a cryopreserved stabilate of infected RBC  
90 (iRBC) is produced from a donor volunteer, enabling subsequent direct blood-stage inoculation of other  
91 volunteers with small numbers of parasites. This model is more practical in non-endemic settings;  
92 enables access to the parasite's genetic data before CHMI; removes all risk of relapsing infection; and  
93 enables multiple studies with the same strain of parasite (for which a safety database can be  
94 established). In the case of *P. falciparum*, this model has also proved particularly suitable for estimating  
95 the blood-stage parasite multiplication rate (PMR) (16) and for enabling experimental transmission to  
96 mosquitoes (17), as compared to studies initiated by mosquito-bite. The blood-stage model is also  
97 advantageous because it extends the period of blood-stage infection, allowing for longer studies of the  
98 human immune response and also switching/selection of parasite variant surface antigens (18).

99 Two cryopreserved stabilates of blood-stage *P. vivax* have been reported to-date, both produced by the  
100 group at the QIMR Berghofer Medical Research Institute, Australia and obtained from returning  
101 travellers who donated infected blood prior to treatment. The first isolate, HMPBS-*Pv* from the Solomon  
102 Islands, was safely tested by blood-stage CHMI in eight volunteers (19, 20), however this necessitated  
103 recruitment of individuals with blood group A to match that of the donor. The second *P. vivax* isolate,  
104 HMP013-*Pv*, was from India and a blood group O+ donor. This has been tested in healthy adult  
105 volunteers and showed successful induction of gametocytemia and experimental transmission of *P.*  
106 *vivax* from humans to mosquitoes (21), and also enabled trials of candidate drugs and further  
107 methodology development (22, 23).

108 Here we take a significant step forward for *P. vivax* CHMI by establishing a well-characterized Thai clone  
109 of *P. vivax* suitable for both mosquito-bite and blood-stage CHMI. We elected to produce a

110 cryopreserved stabilate of iRBC from blood donated by healthy volunteers infected via mosquito-bite  
111 CHMI, as opposed to using a blood donation from a returning traveller. This provided numerous  
112 advantages in terms of logistical timing, and our ability to recruit in advance volunteers who passed a  
113 full health screen and who had universal donor blood group. In real-time we were able to select  
114 mosquitoes infected in Thailand with a single *P. vivax* genotype, thus avoiding production of a  
115 cryopreserved iRBC stabilate from a polyclonal infection. It also minimized the time from mosquito to  
116 blood bank (compared to infected returning travellers); this is important as it has previously been shown  
117 that mosquitoes reset parasite virulence and expression of variant surface antigens (24). Following  
118 production of the cryopreserved parasite stabilate, which we called "PvW1", we demonstrated safety  
119 and infectivity by blood-stage CHMI in six healthy adults, and we also report a full genomic analysis of  
120 the new PvW1 clone.

## 121 **Results**

### 122 **Source patient case-finding and preparation of infected mosquitoes**

123 For infection of mosquitoes, source patients were recruited from a medical clinic in southern Thailand.  
124 Patient blood samples that tested positive for *P. vivax* and negative for filarial disease were fed to  
125 *Anopheles dirus* mosquitoes via a direct membrane feeding system in Thailand. Oocyst and sporozoite  
126 counts subsequently confirmed successful production of three independent batches of infected  
127 mosquitoes (**Figure S1A**). In parallel, and in real-time, source patient samples underwent additional and  
128 rigorous testing in the UK for blood-borne infections and mosquito-borne diseases other than malaria;  
129 all tests were negative. Nested PCR reported mono-infection with *P. vivax* (**Figure S1B,C**), thus  
130 confirming the diagnosis in Thailand, however, genotyping analysis suggested that only one blood  
131 sample (C05-001) contained a single *P. vivax* genotype (**Figure S1A**). Mosquitoes fed off this patient's  
132 blood were therefore selected and shipped from Thailand to the UK.

### 134 **Screening of healthy UK volunteers for blood donation**

135 In parallel we enrolled two healthy UK adult volunteers into the VAC068 clinical trial (**Figure S2**). These  
136 volunteers were specifically screened to be universal blood donors (blood group O rhesus-negative),  
137 Duffy-blood group positive (7, 25); G6PD normal (26); and to have a CYP2D6 genotype predicted to be  
138 an extensive metabolizer phenotype (27) alongside satisfactory demonstration of primaquine  
139 metabolism following administration of a single test dose of drug (13) (**Table S1, Figure S3**). Each  
140 volunteer also underwent an extensive screen for blood-borne infections; all test results were negative,  
141 except both participants were IgG seropositive for Epstein-Barr virus (EBV) and cytomegalovirus (CMV)  
142 (**Table S1**), indicating past infection. However, we did not exclude volunteers based on their serostatus  
143 for these two viruses.

### 145 **Mosquito-bite CHMI – safety and parasite growth dynamics**

146 For the C05-001 mosquito batch, the mean [range] number of oocysts per mosquito was 3 [0-6] at day 7  
147 post-feeding and the median score for number of sporozoites observed in the salivary glands at day 14  
148 post-feeding was +2 (defined as >10-100 sporozoites) (**Figure S1A**). This was relatively low but agreed to  
149 be sufficient for human transmission. Subsequently, the two healthy UK adult volunteers screened and  
150 consented to take part in VAC068 were each exposed to five “infectious bites” as defined post-skin

151 feeding by microscopic examination of each mosquito. To achieve this, volunteers 01-004 and 01-008  
152 required 17 and 33 mosquitoes, respectively, to bite their arm.

153 Parasites were first reliably detected in the blood of both volunteers by qPCR at the evening clinic visit 8  
154 days post-CHMI (dC+8.5), and parasitemia then steadily rose over time (**Figure 1A, Table S2**). Over the  
155 course of the CHMI period, the two volunteers experienced a range of solicited adverse events (AEs),  
156 with both reporting grade 3 fatigue and at least grade 2 anorexia, chills, feverishness, headache,  
157 malaise, nausea and sweats (**Figure 1B**). Both volunteers were admitted for blood donation when they  
158 met protocol-specified criteria defined by symptoms and or threshold levels of parasitemia as measured  
159 in genome copies (gc)/mL by qPCR. This occurred on the morning of dC+14 for both volunteers, who  
160 both crossed the 10,000 gc/mL threshold on dC+13.5 and developed fever on dC+14. Following  
161 admission to the clinical trials unit, a 250 mL blood sample was collected (at dC+14 for volunteer 01-008  
162 and dC+14.5 for volunteer 01-004); both were positive by thick film microscopy and reported 16,717 or  
163 31,010 gc/mL by qPCR, respectively. Prior to cryopreservation, these blood samples were then  
164 randomized and relabelled either “Donor 1” or “Donor 2” and are now referred to as such in the Results.

165 After blood donation, each volunteer was immediately treated with Riamet® followed by a 14-day  
166 course of primaquine; no supportive treatment or hospital admission was required for either volunteer.  
167 Monitoring by qPCR on days 1, 2, 4, 10 and 16 post-treatment showed a rapid decline in blood-stage  
168 parasitemia followed by negative readings for both volunteers (**Figure 1A, Table S2**). Most solicited  
169 symptoms increased in severity in the first 24 hours after starting anti-malarial treatment (**Figure S4A**).  
170 Objective fever also increased in the 24 hours post-treatment (**Figure 1C**), and one volunteer developed  
171 a grade 3 pyrexia (**Figure S4B**), but all symptoms had completely resolved within 5 days of starting  
172 treatment. Both volunteers also experienced some short-lived grade 1 or 2 AEs possibly related to the  
173 anti-malarial treatment (dizziness, insomnia and abdominal pain) (**Figure S4C**). Very few unsolicited AEs  
174 (at least possibly related to CHMI) were reported by either volunteer (**Table S3A**), and only one grade 3  
175 unsolicited AE (migraine, not related to CHMI) was reported by 01-004 more than 2 months post-  
176 challenge, requiring attendance to their doctor and resolving within 48 hours (**Table S3B**). Lymphocyte  
177 and platelet counts dropped in both volunteers around the time of blood donation (platelets remained  
178 within the normal range but both developed a grade 2 lymphocytopenia), rising back to pre-challenge  
179 levels within 48 hours (**Figure 1D-E and Table S3C**). Volunteer 01-008 also developed a transient grade 1  
180 anemia ~6 weeks post-challenge (123 g/L at dC+47) which may or may not have been related to CHMI,  
181 but this resolved within 3 months (131 g/L at dC+94).

182 Following completion of the study, the parasite multiplication rate (PMR) for both volunteers was  
183 calculated using a linear model fitted to  $\log_{10}$ -transformed qPCR data (28). These data showed  
184 comparable PMRs in both volunteers, with 10.7- and 11.5-fold growth per 48 hours (**Figure 1G**). We also  
185 analysed gametocytemia using a qRT-PCR assay to detect mature female gametocyte *pvs25* transcripts.  
186 Volunteer 01-004 showed only low levels at the final time-point pre-treatment (dC+14.5) whilst none  
187 were detected in volunteer 01-008 (**Figure 1H**).

188 Finally, with regard to longer-term safety monitoring, clinic visits at dC+45 and dC+90 gave rise to no  
189 safety concerns or indication of relapsing infection, and repeat serological tests for blood-borne  
190 infections at dC+90 all remained negative. Ongoing annual follow-up by email will continue for 5 years  
191 post-CHMI, however, as of time of writing (3 years post-primaquine treatment) no relapse of *P. vivax*  
192 has been diagnosed for either volunteer (see **Supplementary Text**).

193

#### 194 **Cryopreservation and *in vitro* testing of *P. vivax* infected blood**

195 After blood donation, the leukodepleted blood from both volunteers in VAC068 was processed, and the  
196 RBC mixed with Glycerolyte 57 to form a stabilate prior to cryopreservation. In total, 190 vials were  
197 frozen for Donor 1 and 185 for Donor 2. In process testing by qPCR indicated minimal or no loss of  
198 parasites during filtration (95% and 105% recovery for Donor 1 and Donor 2, respectively). We next  
199 tested for parasite viability in both cryopreserved stabilates. Vials were thawed and cells used in a short-  
200 term *in vitro* parasite culture assay, given *P. vivax* cannot currently be cultured long-term *in vitro*.  
201 Parasite growth was detectable by qPCR and light microscopy through one initial growth cycle in  
202 samples collected from Donor 1, with normal progression of parasite morphology seen on Giemsa  
203 stained thick and thin blood films (**Figure 2**). However, no growth was discernible in samples obtained  
204 from Donor 2. We therefore undertook further QC testing on vials from Donor 1, with the material  
205 tested for sterility, mycoplasma and endotoxin; all tests were passed. Another screen for blood-borne  
206 infections was also conducted on the plasma derived directly from the blood donation; all tests were  
207 negative.

208

209 Finally, we also screened Donor 1 for the Kell blood group antigen because women of childbearing  
210 potential that receive a blood transfusion have a small additional risk of developing RBC alloantibodies  
211 that could cause problems during pregnancy. In particular, there is a potential risk of development of

212 hemolytic disease of the newborn in relation to Kell antigen incompatibility, i.e. if Kell-positive donor  
213 blood is transfused to a Kell-negative female recipient. However, testing of the donor's blood sample  
214 confirmed Kell antigen negativity, thereby allowing future universal administration of the cryopreserved  
215 *P. vivax* iRBC stabilate with respect to gender.

216

### 217 **Blood-stage CHMI – PvW1 infectivity, parasite growth dynamics and safety**

218 Given all safety and viability tests were passed for the cryopreserved stabilate of *P. vivax* iRBC from  
219 Donor 1, we named this clonal isolate “PvW1” and proceeded to test safety and infectivity by blood-  
220 stage CHMI. We therefore recruited six healthy, malaria-naïve UK adults into the VAC069A clinical trial,  
221 comprising three groups of two volunteers (**Figure S5**), and tested feasibility of infection at three  
222 different doses of PvW1 blood-stage inoculum. Five vials of the PvW1 cryopreserved stabilate were  
223 thawed and then combined to produce a single batch of blood-stage inoculum. Two volunteers receive a  
224 whole vial's worth of iRBC (“neat”), two volunteers received one fifth of the challenge dose via a 1:5  
225 dilution, and the final two volunteers were inoculated with one twentieth of the dose via a 1:20 dilution.  
226 All six volunteers underwent blood-stage CHMI at the same time.

227 Blood-stage parasitemia was monitored as previously by qPCR, beginning one day after challenge (dC+1)  
228 (**Figure 3A, Table S4**). All six volunteers were successfully infected, with a median time to diagnosis of  
229 15.25 days post-CHMI (range 12.5-16.5) (**Figure 3B**). The median (range) parasitemia at diagnosis across  
230 all six volunteers was 9,178 (3,779 – 17,795) gc/mL (**Figure 3C**). We also calculated the PMR as before  
231 using a linear model fitted to log<sub>10</sub>-transformed qPCR data (28). These data showed a median (range) of  
232 5.7 (3.6 – 7.0)-fold growth per 48 hours across the six volunteers (**Figure 3D**), notably lower than that  
233 previously observed in the mosquito-bite CHMI study (**Figure 1F**). There was also no discernible  
234 difference in the PMRs across the three different challenge dose cohorts (**Figure 3D**); or across the three  
235 different Duffy blood group sero-phenotypes, all with median values between 5.3 – 5.9-fold growth per  
236 48 hours (**Figure 3E**). We also analysed gametocytemia at the six time-points preceding diagnosis for  
237 each volunteer, and observed rising levels in all individuals (**Figure 3F**). This was in clear contrast to the  
238 observations post-mosquito bite CHMI (**Figure 1G**) and despite comparable (if not slightly lower) levels  
239 of overall blood-stage parasitemia as measured in gc/mL. Here, we also saw a strong positive correlation  
240 between the measured overall levels of parasitemia in gc/mL versus *pvs25* transcripts/μL (**Figure 3G**).

241 With regards to safety, there were no serious adverse events (SAEs) in the VAC069A study and all  
242 volunteers completed treatment without complication. One volunteer withdrew at dC+28, with the  
243 remaining five completing clinical follow-up at dC+90 (**Figure S5**). The maximum severity of solicited AEs  
244 at any time during the CHMI period is shown for all six volunteers in **Figure 4A**, with four volunteers  
245 reporting grade 3 solicited AEs (most commonly feverishness) persisting for 24 hours and one for 48  
246 hours (**Table S5A**). The proportion of volunteers reporting solicited AEs specifically pre-diagnosis, peri-  
247 diagnosis and post-treatment is shown in **Figure 4B**. Around the time of diagnosis, 33-50% of the  
248 volunteers reported mild-to-moderate symptoms; mainly fatigue, headache, myalgia, malaise,  
249 feverishness and chills. Symptoms peaked in severity in the first 24 hours after starting anti-malarial  
250 treatment with Riamet® or Malarone, with only one volunteer remaining asymptomatic (**Figure 4B**).  
251 Objective fever also increased in the 24 hours post-treatment, with 3/6 volunteers developing pyrexia,  
252 one of each grades 1-3 (**Figure 4C, Figure S6A**). Nevertheless, most symptoms had completely resolved  
253 within a few days of starting treatment and only one volunteer still had headache and fatigue at 6 days  
254 post-starting treatment (T+6) (**Figure 4B**). Three volunteers (50%) also experienced short-lived AEs  
255 possibly related to the anti-malarial drugs (50% moderate dizziness, 33% mild insomnia, cough and  
256 palpitations) (**Figure S6B**). Very few unsolicited AEs (at least possibly related to CHMI) were reported by  
257 any of the volunteers (**Table S5B**).

258 With regard to laboratory AEs (**Table S5C**), lymphocyte counts dropped significantly in 4/6 volunteers  
259 around the time of diagnosis or 1 day post-treatment (grade 3 lymphocytopenia in two volunteers), but  
260 all counts normalized within 6 days of starting treatment (**Figure 4D**). Two volunteers developed a short-  
261 lived grade 2 thrombocytopenia, again normalizing within 6 days of treatment (**Figure 4E**); whilst two  
262 volunteers also developed a mild-moderate anaemia post-diagnosis. With regards to the latter, one  
263 normalized within 28 days of challenge, the other persisted at grade 1 at dC+90 (102 g/L) and so was  
264 referred to their medical practitioner for ongoing monitoring as a precautionary measure (**Table S5C** and  
265 **Figure S6C**). The only notable change in blood chemistry was a transient grade 1-2 rise in the ALT in 4/6  
266 volunteers, captured consistently at 6 days post-treatment (**Figure 4F**). All fully resolved to pre-challenge  
267 levels with no associated abnormalities in other indices of liver function (**Figure S6C, Table S5D**). Finally,  
268 we also confirmed CMV and EBV sero-status of all volunteers pre- and post-CHMI. All six volunteers  
269 were EBV sero-positive pre-CHMI and three were CMV sero-positive. Of the three CMV sero-negative  
270 volunteers, one withdrew consent and left the trial at C+28 and was therefore not re-tested, whilst the  
271 other two remained sero-negative when re-tested at C+90.

272

**273 Antibody responses to blood-stage merozoite antigens post-CHMI**

274 We next assessed for the induction of serum IgG antibody responses post-CHMI against two well-known  
275 blood-stage merozoite antigens – *P. vivax* merozoite surface protein 1 C-terminal 19 kDa region  
276 (PvMSP1<sub>19</sub>) and *P. vivax* Duffy-binding protein region II (PvDBP\_RII). All volunteers had detectable IgG  
277 against PvMSP1<sub>19</sub> post-CHMI, with similar results seen in the VAC068 mosquito-bite sporozoite CHMI  
278 study and the VAC069A blood-stage CHMI study (**Figure 5A**). However, there were no detectable  
279 responses post-CHMI against PvDBP\_RII in any of the volunteers, in contrast to positive control samples  
280 from a cohort of healthy UK adult volunteers previously vaccinated with the PvDBP\_RII antigen (29)  
281 which were included here for comparison (**Figure 5B**). We also assessed for the induction of serum IgG  
282 antibody responses post-CHMI against the well-known pre-erythrocytic antigen, *P. vivax*  
283 circumsporozoite protein (PvCSP). Responses were negative pre-CHMI in both VAC068 volunteers, with  
284 no evidence of seroconversion to PvCSP at dC+90 post-sporozoite CHMI (data not shown).

285

**286 PvW1 genome assembly allows resolution of complex multi-gene families**

287 Finally, we produced a genome assembly for PvW1 by using a hybrid assembly method which combined  
288 long PacBio reads with short Illumina reads. The PvW1 genome assembled into 14 scaffolds (the 14 *P.*  
289 *vivax* chromosomes), and is comparable in both assembly size and number of genes to the highest  
290 quality existing *P. vivax* assembly, PvP01 (30) (**Table 1**). The PvW1 assembly has fewer unassigned  
291 scaffolds than any other assembly, indicating the completeness of the assembled genome and the  
292 benefits of using a combination of long and short reads; note the PvP01, PvC01 and PvT01 were all  
293 assembled using Illumina data only (30), while the original reference, PvSalvador-1 (Sall), was created  
294 using capillary sequence data (31).

295 The high quality of the PvW1 assembly allowed us to identify 1145 *Vivax* interspersed repeat (VIR) genes  
296 within the genome, comparable in number to the PvP01 genome. Computational studies have shown  
297 that the VIR genes from different *P. vivax* isolates can be grouped into a number of clusters, and it is  
298 possible that genes within clusters may be performing a similar function (30, 32). Cluster analysis  
299 showed that the majority of the 1145 PvW1 VIR proteins could be clustered into groups with VIRs from  
300 the PvP01, PvT01, PvC01 and Sall strains (**Figure 6**), with no evidence that specific clusters are restricted  
301 to specific genomes or geographical regions. Of 206 vir clusters that had >5 genes, and therefore had  
302 the potential to include vir representatives from all five isolates, 98 were missing at least one isolate.

303 However, in 90 of those cases, the missing isolate was Sall. As shown in **Table 1**, the Sall genome, which  
304 was sequenced more than ten years ago using earlier genome sequencing technology, has significantly  
305 fewer vir genes, presumably because such genes are concentrated in subtelomeric regions which are  
306 largely unassembled in that genome. There were only 24 clusters that were missing at least one isolate  
307 from the more fully assembled genomes (PvW01, PvT01, PvC01 and PvP01); if the size of the clusters  
308 was increased to greater than 8 genes, that number of clusters missing at least one isolate dropped to 9.  
309 This emphasises that the vast majority of clusters appear to be present across genomes and geographic  
310 regions, raising the hypothesis that the clusters may have primarily emerged before the broad  
311 geographic dispersal of *P. vivax*. Similarly, we resolved other smaller but still highly polymorphic  
312 multigene families such as the merozoite surface protein 3 (MSP3) family. These proteins are expressed  
313 on the surface of the invasive merozoite and are known to be highly polymorphic both in sequence and  
314 gene number between isolates. We compared the organization of the MSP3 multigene family in PvW1  
315 to *P. vivax* isolates: PvP01 (30) and Sall, India-7, North Korean, Mauritania-1 and Brazil-1 (33). Genes  
316 flanking the MSP3 cluster (PVX\_097665 and PVX\_097740) are syntenic across all isolates, as are MSP3.1,  
317 MSP3.2, MSP3.3, MSP3.G, MSP3.10 and MSP3.11. There is however clearly variability in the central  
318 region of the MSP3 region, with MSP3.4, MSP3.5, MSP3.6, MSP3.7, MSP3.8 and MSP3.9 all present in  
319 some isolates but not others (**Figure S7**). The arrangement of the PvW1 MSP3 cluster appears identical  
320 to that of PvP01.

321

### 322 **PvW1 vaccine candidate and drug resistance associated genes**

323 The quality of the PvW1 genome also makes it easy to obtain and analyze potential vaccine targets,  
324 which we did for three high profile candidates (34), comparing the PvW1 sequence with those from  
325 PvP01 and Sall. The sporozoite-stage target PvCSP is known to contain one of two major types of repeat  
326 called VK210 and VK247 (35, 36), with this heterogeneity an important factor for vaccine design. PvW1  
327 contains VK210 repeats, the most prevalent form worldwide (**Figure S8A**). The sequence of the  
328 transmission-stage candidate Pvs25 is highly conserved between PvW1 and other genomes, apart from  
329 the commonly variable amino acids 130 and 131 within the third epidermal growth factor (EGF)-like  
330 domain (**Figure S8B**). Finally, we reviewed the PvDBP sequence given two vaccine candidates targeting  
331 region II are currently in early-phase clinical trials (29, 37). PvDBP in PvW1 has multiple polymorphisms  
332 with 10 in region II, including the DEK epitope (38), as compared to the Sall sequence used in the current  
333 clinical vaccines (29, 37). Like PvDBP from Sall, this gene in PvW1 also has a nine amino acid deletion

334 (downstream of region II) that is not present in PvP01 (**Figure S8C**). As well varying at a sequence level,  
335 PvDBP is also known to vary between isolates in copy number, with some isolates containing multiple  
336 copies (39, 40) now linked to evasion of humoral immunity (41). We therefore used Illumina read  
337 mapping across the PvW1 genome assembly to check for copy number variation of genes. Here, if  
338 regions of the genome are present in multiple copies then the read coverage over that region would be  
339 higher than the surrounding regions. There was no evidence for increased coverage at either PvDBP or  
340 its homologue PvDBP2 (also called *P. vivax* erythrocyte-binding protein, PvEBP), suggesting both are  
341 present at a single copy within the PvW1 genome (**Figure S9A-B**). We also looked at an uncharacterized  
342 gene on chromosome 14, homologous to PVX\_101445 / PvP01\_1468200, which has been shown to be  
343 duplicated in some isolates (42). This gene is also present in a single copy in PvW1 (**Figure S9D**).

344 Drug resistance is not as well characterized in *P. vivax* as in *P. falciparum*, but several genes and  
345 polymorphisms have been associated with resistance in field studies. We therefore examined the  
346 sequences of four genes within the PvW1 genome that have been associated with drug resistance:  
347 dihydrofolate reductase (*PvDHFR*), dihydropteroate synthetase (*PvDHPS*), chloroquine resistance  
348 transporter (*PvCRT*) and multidrug resistance transporter 1 (*PvMDR1*). The PvW1 *PvDHFR* gene encodes  
349 a protein with the quadruple mutation F57L/S58R/T61M/S117T that has been linked to pyrimethamine  
350 resistance (43), whereas *PvDHPS* showed no mutations previously associated with sulfadoxine resistance  
351 (44). The molecular basis of *P. vivax* chloroquine resistance is less clear, although there is some evidence  
352 that mutations in *PvCRT* (K10 insertion) and *PvMDR1* (Y976F mutation) may be involved (45-47). Neither  
353 of these mutations are present in the PvW1 *PvCRT* and *PvMDR1* genes. It is important to note that both  
354 Riamet® (a combination of artemether and lumefantrine) and Malarone (a combination of atovaquone  
355 with proguanil) antimalarials were used with 100% treatment success rates in the VAC068 and VAC069A  
356 studies (both volunteers in VAC068 and 5/6 volunteers in VAC069A received Riamet®, 1/6 received  
357 Malarone), and none of the polymorphisms identified have been associated with resistance to either of  
358 these drugs.

## 359 Discussion

360 Here we undertook CHMI model development for *P. vivax* and established a new PvW1 clonal isolate  
361 from Thailand. Our methodology elected to focus on a mosquito-bite CHMI protocol to provide the  
362 initial source of blood-stage parasites for the cryopreserved stabilate. The main advantages here (over  
363 parasites donated by returning travellers) included the ability to control the parasite source, the  
364 recruitment of suitable healthy volunteers (especially with regard to health screening and universal  
365 donor blood group) and logistical timing. We also created the blood stabilate as close as possible to the  
366 mosquito-stage, with only ~3 cycles of replication from the liver (given it is known that mosquitoes reset  
367 parasite virulence (24)). If parasites had been cryopreserved from returning travellers or chronically-  
368 infected adults in an endemic setting they would have been selected over many rounds of asexual  
369 replication *in vivo* before creating the stabilate. This diminishes the criticism that blood-stage CHMI is  
370 not the natural route of infection. Furthermore, as many as 80% of *P. vivax* blood-stage infections are  
371 caused by relapsing parasites, which means that in the unique context of relapsing *P. vivax*, a challenge  
372 with recently emerged blood-stages is in many ways closer to most “natural challenges” than mosquito  
373 bite-delivered sporozoites. That being said, it is important to acknowledge that blood-stage CHMI is only  
374 useful to measure interventions against the blood-stage of infection rather than sporozoites or  
375 hypnozoite establishment.

376 Notably our real-time assessment of parasite genotypes in the infected mosquitoes in Thailand  
377 identified only one clonal infection out of three tested. In future it will likely be necessary to screen  
378 more infected patient samples if parasite clones with specific genotypes are desired. It is also probable  
379 that this clonal infection resulted from a single relapsing hypnozoite in the patient, given natural  
380 infections are frequently polyclonal, arising from primary infections with multiple genotypes and meiotic  
381 siblings produced in the mosquito and/or multiple heterologous hypnozoites relapsing at a similar time  
382 (48-50).

383 The VAC068 mosquito-bite trial demonstrated feasibility and safety of this CHMI model for the first time  
384 at a European site, albeit in only two healthy adult UK volunteers. Both were successfully infected, with  
385 parasites first detectable by qPCR on dC+8.5 and the first wave of blood-stage parasitemia peaking  
386 around dC+9. This is largely consistent with data from humanized mouse models suggesting that the  
387 complete maturation of *P. vivax* liver stages and exo-erythrocytic merozoite release occurs between  
388 days 9 and day 10 post-sporozoite infection (51). Growth of blood-stage parasitemia was subsequently

389 similar in the two volunteers, with both meeting criteria to donate blood on dC+14, prior to radical cure  
390 treatment with Riamet® followed by primaquine. Both volunteers were screened to have CYP2D6  
391 genotypes predicted to be extensive metabolizer phenotypes of primaquine, and as of ~3 years' long-  
392 term follow-up, no relapse of infection has been documented.

393 Cryopreservation of the iRBC stabilate was performed successfully, however, given *P. vivax* cannot be  
394 cultured long-term *in vitro* it proved challenging to confirm parasite viability following thaw of the  
395 frozen stabilate, especially given the relatively low level of parasitemia achieved by CHMI in non-  
396 immune adults. However, given the stabilate from Donor 1 showed demonstrable growth *in vitro* using a  
397 short-term culture assay, we elected to proceed with this material for onward testing. Poor parasite  
398 recovery from Donor 2 could be associated with the predominant lifecycle stage at the time of  
399 cryopreservation; here microscopy records indicated the presence of more schizonts and a smaller  
400 proportion of early ring-stage trophozoites in comparison to Donor 1. Previous evidence suggests that  
401 the late asexual intra-erythrocytic parasites are not viable after cryopreservation with glycerolyte (52),  
402 and this may have led to the poor recovery of live parasites in Donor 2's stabilate.

403 Previous reports of blood-stage CHMI using *P. vivax* have used one vial of cryopreserved stabilate to  
404 infect one volunteer (19-21), in contrast to similar studies with the stabilate of 3D7 clone *P. falciparum*  
405 whereby a single vial is diluted and routinely used to infect ~20-30 volunteers (16, 53). Thawing many  
406 vials to undertake CHMI in larger cohorts of volunteers, e.g. for vaccine efficacy trials, brings many  
407 practical difficulties and, in turn, more rapidly depletes the bank of cryopreserved stabilate which is a  
408 finite resource. Conserving vials and building up a long-term safety database of the challenge agent for  
409 future use across many clinical studies is also preferable. Consequently, we assessed three different  
410 doses of the PvW1 blood-stage inoculum in the VAC069A study, with two volunteers receiving each  
411 dose. All six volunteers were successfully diagnosed at similar levels of blood-stage parasitemia within  
412 12-16 days. Importantly, these data suggest that blood-stage CHMI trials in larger volunteer cohorts are  
413 now practical and feasible, whilst preserving the bank of PvW1 parasites for the long-term.

414 The AE profiles of both the mosquito-bite and blood-stage CHMI with PvW1 were highly comparable to  
415 previous reports of both models in malaria-naïve/non-immune adults using other isolates of *P. vivax* at  
416 the Colombian (8-10), American (54) or Australian sites (19-23). No SAEs occurred in either trial and all  
417 drug treatments were successful. Symptoms consistent with malaria were experienced and peaked post-  
418 treatment prior to resolving within a few days. We also observed transient thrombocytopenia and  
419 lymphocytopenia, as well as rises in ALT six days post-treatment, consistent with the reports of other

420 sites undertaking *P. vivax* CHMI (9, 10, 55) and with no apparent impact on volunteer safety. We also  
421 observed consistent sero-conversion to PvMSP1<sub>19</sub> post-CHMI in all volunteers, as reported in the  
422 Colombian CHMI trials (10, 56), but no detectable responses to PvDBP\_RII or PvCSP. These data for the  
423 merozoite antigens are in line with our similar studies of *P. falciparum* CHMI, with sero-conversion of  
424 malaria-naïve adults observed to immuno-dominant merozoite surface proteins following primary acute  
425 malaria exposure, but not to more transiently exposed RBC invasion ligands (57, 58).

426 Following mosquito-bite CHMI we observed ~10-fold growth in blood-stage parasitemia per 48 hours,  
427 consistent with other reports for *P. vivax* (20), as well as our experience with *P. falciparum* (16, 53).  
428 Interestingly, however, the average PMR was lower (~5.5-fold growth per 48 hours) following blood-  
429 stage CHMI with the same parasite. There was no obvious effect of challenge dose or Duffy blood group  
430 sero-phenotype on the PMR, the latter consistent with our observations *in vitro* using *P. knowlesi*  
431 parasites transgenic for PvDBP (59). However, Duffy blood group sero-phenotype has been linked to  
432 susceptibility of *P. vivax* clinical malaria following natural infection (60). Consequently CHMI studies in  
433 larger numbers of volunteers will be required to more stringently assess for any relationships between  
434 blood group antigens and the observed PMR, and to more accurately establish the natural variability in  
435 the PMR observed in malaria-naïve adults. A second striking difference between the two CHMI models  
436 was the apparent minimal gametocytemia following mosquito-bite CHMI, in contrast to blood-stage  
437 CHMI. In the latter, the *pvs25* transcripts (a marker of mature female gametocytes) were reliably  
438 detected in all six volunteers, reaching comparable levels to those reported in other *P. vivax* blood-stage  
439 CHMI studies (19, 20). Notably, poor transmission to mosquitoes was reported in another *P. vivax*  
440 mosquito-bite CHMI trial, consistent with our data here (61). Interestingly, a more recent study  
441 comparing the same two CHMI models with *P. falciparum* reported the same finding (17). Why blood-  
442 stage CHMI appears to lead to much greater gametocytemia than mosquito-bite CHMI, despite reaching  
443 comparable levels of overall parasitemia by the time of diagnosis, remains to be determined. However,  
444 this might reflect the greater number of asexual growth cycles since liver egress, or a longer time to  
445 diagnosis allowing for an extended window for conversion of asexual parasites.

446 Finally, we proceeded to undertake a genomic analysis of the new *P. vivax* PvW1 clone. The need to  
447 drug treat volunteer infections at relatively low parasitemia limited the amount of PvW1 parasite DNA  
448 that could be isolated for sequencing. Nevertheless, a very high quality genome assembly for PvW1 was  
449 created by using a hybrid assembly method which combined long PacBio reads with short Illumina  
450 reads. The PacBio library was created using low-input PacBio technology developed to create a genome

451 assembly from a single mosquito (62), and is to our knowledge the first time that this has been applied  
452 to *Plasmodium* parasites. Our goal is that the PvW1 clone will become a valuable tool for vaccine  
453 discovery, drug testing and assessment of *P. vivax in vivo* immuno-biology. Accurate assessment of both  
454 the sequence and copy number of vaccine candidate antigens within the PvW1 genome will thus be  
455 critical in designing future vaccine immunogens and interpreting CHMI efficacy studies. The high quality  
456 of the PvW1 assembly allowed us to easily report on leading vaccine candidate antigens, analyze genes  
457 and polymorphisms associated with drug resistance in field studies, and resolve 1145 VIR genes as well  
458 as the smaller polymorphic PvMSP3 multigene family. Although the function of the highly variable  
459 subtelomeric multigene VIR family is not well defined, related genes are found in high numbers in most  
460 *Plasmodium* species which infect humans, monkeys and rodents, and some are thought to be involved  
461 in immune evasion, including by directly binding to and down-regulating natural killer (NK) cell ligands  
462 (63). Our cluster analysis will now enable comparison of gene function within and between clusters, and  
463 should help in the future elucidation of the function of the VIR gene family.

464 In conclusion, we have developed a mosquito-transmitted stabilate using a new clonal field isolate of *P.*  
465 *vivax* and combined new methodologies for parasite isolation and ultra-low input PacBio sequencing to  
466 assemble a reference-quality genome for CHMI. This has i) revealed polymorphisms in leading drug and  
467 vaccine targets that can now be functionally tested *in vivo* with PvW1 and ii) used a hybrid  
468 PacBio/Illumina genome assembly technique to identify 1145 unique VIR genes. This will allow for *in vivo*  
469 switching and selection of multi-gene families to be measured in *P. vivax* in the same way as has been  
470 done for *P. falciparum* (18). This has allowed us to open up many new research avenues, and in the first  
471 instance, we have used this model to investigate myeloid cell activation, systemic inflammation, and the  
472 fate and function of human T cells during a first-in-life *P. vivax* infection (64). The PvW1 parasite should  
473 prove to be an invaluable resource for the wider malaria community.

474 **Methods**

475

476 Detailed methods are provided in **Supplementary Methods**. In brief:

477

478 **Study design.** VAC068 was a clinical study to assess the safety of controlled human *P. vivax* malaria  
479 infection through experimental sporozoite inoculation (by mosquito-bite) of healthy malaria-naïve UK  
480 adults. The study was conducted in the UK at the Centre for Clinical Vaccinology and Tropical Medicine  
481 (CCVTM), University of Oxford (recruitment, follow-up post-CHMI, admission for blood donation and  
482 treatment) and at the Sir Alexander Fleming Building (Infection and Immunity section) Imperial College  
483 of Science, Technology and Medicine, London (sporozoite challenge of volunteers, delivered by  
484 mosquito bite in the designated category 3 suite). Concurrent primary objectives of the trial were to  
485 assess the immune response to primary *P. vivax* infection and to assess gametocytemia following  
486 infection. Secondary objectives were to obtain up to 250 mL of blood from each infected volunteer and  
487 produce a cryopreserved stabilate of iRBC for future use in blood-stage *P. vivax* CHMI studies. VAC068  
488 volunteers were admitted to the CCVTM in Oxford according to a clinical / diagnostic algorithm.  
489 Following admission, a 250 mL blood sample was collected using aseptic technique, via a whole blood  
490 donation kit containing an in-line leukodepletion filter (Leukotrap WB, Haemonetics Corp), at room  
491 temperature. Antimalarial treatment (60-hour course of artemether/lumefantrine, Riamet®) was started  
492 immediately after blood donation, followed by a 14-day course of primaquine, 30 mg once daily. Follow-  
493 up was out to 5 years to monitor for any signs of relapse. The VAC069A study assessed the safety and  
494 infectivity of blood-stage *P. vivax* CHMI in healthy malaria-naïve UK adults, through experimental  
495 inoculation with the cryopreserved PvW1 infected erythrocytes collected from Donor 1 in VAC068, at  
496 three different doses. The PvW1 blood-stage inoculum was thawed and prepared under strict aseptic  
497 conditions as previously described for *P. falciparum* (16), with some modifications. All six volunteers  
498 were challenged (two receiving each dose dilution) and followed up at the CCVTM, Oxford, UK.  
499 Diagnostic criteria were based on thick blood film microscopy results and qPCR in the presence or  
500 absence of symptoms. Treatment was completed with either a 60-hour course of Riamet® or a 48-hour  
501 course of Malarone and volunteers followed up for 90 days. Full details of diagnostic criteria and follow-  
502 up schedules for both studies, case-finding in Thailand and preparation of infected mosquitoes for  
503 transfer to the UK, are described in **Supplementary Methods**.

504 **Participants.** Healthy, malaria-naive males and non-pregnant females aged 18-50 were invited to  
505 participate in the study. Two and six volunteers were enrolled for each respective trial in total. A full list  
506 of inclusion and exclusion criteria and specific considerations for screening of healthy UK adult  
507 volunteers for the VAC068 study are reported in **Supplementary Methods**.

508 **Safety analysis.** Data on both solicited AEs occurring during and after the CHMI period (that may have  
509 related to CHMI or antimalarial treatment) as well as any unsolicited AEs, were collected at clinic visits,  
510 from dC+1 up until the end of primaquine antimalarial treatment (VAC068) and until 6 days post-  
511 initiation of Riamet<sup>®</sup>/Malarone treatment (VAC069A). Volunteers were given a card on which to  
512 document the end date of any outstanding malaria symptoms on-going between completing anti-  
513 malarial therapy and their next clinic visit. Data on SAEs were collected throughout the entire study  
514 period. Details on assignment of severity grading and causality are provided in the **Supplementary**  
515 **Methods**.

516 **Total parasite quantification.** Quantitative PCR (qPCR) was used to monitor total *P. vivax* blood-stage  
517 parasitemia in volunteers' blood in real-time. The assay targets the 18S ribosomal RNA (rRNA) gene and  
518 was adapted from previously published methodology (19, 53).

519 **Thick blood film microscopy.** Collection of blood, preparation of thick films and slide reading for VAC068  
520 volunteers were performed according to Jenner Institute Standard Operating Procedure (SOP) ML009.  
521 Briefly, slides were prepared using Field's stain A and then Field's stain B. 200 fields at high power  
522 (1000x) were read. Visualization of two or more parasites in 200 high power fields constituted a positive  
523 result.

524 **Cryopreservation and *in vitro* testing of *P. vivax* infected blood (VAC068).** After blood donation, the  
525 leukodepleted blood from both volunteers was maintained at ~37 °C and transported immediately to  
526 the Jenner Institute Laboratories, University of Oxford. Here, RBC were separated from plasma by  
527 centrifugation before mixing the RBC with Glycerolyte 57 (Fenwal 4A7833) at 1:2 volume ratio. All  
528 procedures were conducted according to SOPs under stringent Quality Assurance (QA) oversight and  
529 guidance from a Qualified Person (QP) at the University of Oxford. The RBC-Glycerolyte mixture was  
530 finally aliquoted at 1.5 mL per cryovial, transferred into CoolCells (Corning 432009) and placed at -80 °C  
531 within 2 h 30 min of blood donation to freeze overnight; the following day the frozen cryovials were  
532 transferred to long-term storage in liquid nitrogen. A final screen for blood-borne infections was

533 conducted on the plasma, derived directly from the blood donation (separated from the RBC prior to  
534 cryopreservation), in line with testing procedures performed by the UK NHS Blood Transfusion service.  
535 RNA PCR for HIV-1 and hepatitis C, DNA PCR for hepatitis B, EBV CMV, and serology for HIV-2, HTLV-1,  
536 HTLV-2, and *Treponema pallidum* was performed on thawed plasma samples at University Hospitals  
537 Birmingham NHS Foundation Trust, UK (Public Health England, Birmingham Laboratory). Separately,  
538 screening of a blood sample from Donor 1 for the Kell blood group antigen was performed by Oxford  
539 University Hospitals NHS Trust Haematology Laboratory, UK. The cryopreserved stabilate from Donor 1  
540 was also tested for sterility by direct inoculation and mycoplasma by specific culture. Finally, endotoxin  
541 was quantified by kinetic chromogenic limulus amoebocyte lysate assay. These assays were conducted  
542 by a Contract Research Organization: SGS Vitrology, Glasgow, UK or SGS Vitrology's contracted services  
543 at Moredun Scientific, Penicuik, Scotland, UK. The tests were non-regulatory standard and performed  
544 for information only.

545 **Gametocyte quantification.** *P. vivax* gametocytemia was determined by one-step quantitative reverse  
546 transcription PCR (qRT-PCR) targeting the messenger RNA marker of female mature gametocytes, *pvs25*.  
547 For RNA extraction samples were processed within 4 h of blood sampling (Qiagen) followed by one-step  
548 RT-PCR using Luna® Universal Probe One-Step RT-qPCR Kit (New England Biolabs).

549 **Modelling of PMR – VAC068 and VAC069A.** A qPCR-derived PMR was modelled based on previously  
550 described methodology (28, 53, 65).

551 **Anti-PvDBP\_RII standardized ELISA.** ELISAs to quantify circulating PvDBP\_RII-specific total IgG responses  
552 were performed using standardized methodology, similar to that previously described (29). Day C-1 and  
553 dC+90 serum or plasma samples from the VAC068 and VAC069A volunteers were tested, alongside  
554 samples from 8 healthy UK adults previously vaccinated in the VAC051 Phase Ia trial of a candidate  
555 PvDBP\_RII vaccine (Group 2C) (29).

556 **Anti-PvMSP1<sub>19</sub> ELISA.** Anti-PvMSP1<sub>19</sub>-specific total IgG responses were measured in VAC068 volunteer  
557 serum or plasma via indirect ELISA (same test samples as for the PvDBP\_RII ELISA).

558 **Illumina and long read sequencing.** DNA was extracted from blood taken from the VAC068 volunteers  
559 at 11 and 14 days post-CHMI using the Qiagen blood DNA midi kit and sequenced with Illumina HiSeq  
560 X10 with 150 bp paired end reads. (See **Supplementary Methods** for details on preparation of schizonts,

561 high molecular weight DNA extraction and Shearing and PacBio library construction and sequencing, and  
562 VIR gene analysis).

563 **Statistics.** Unless otherwise stated, data were analyzed using GraphPad Prism version 9.1.1 for Windows  
564 (GraphPad Software Inc.). All tests used were 2-tailed and are described in the text. A value of  $P < 0.05$  was  
565 considered significant.

566 **Study approvals.** The VAC068 and VAC069 trials were registered on ClinicalTrials.gov (NCT03377296 and  
567 NCT03797989, respectively) and were conducted according to the principles of the current revision of  
568 the Declaration of Helsinki 2008 and in full conformity with the ICH guidelines for Good Clinical Practice  
569 (GCP). All volunteers signed written consent forms, and consent was checked to ensure volunteers were  
570 willing to proceed prior to CHMI. The VAC068 study received ethical approval from the UK NHS Research  
571 Ethics Service (Oxfordshire Research Ethics Committee A, Ref 17/SC/0389). The VAC069 study received  
572 ethical approval from the UK NHS Research Ethics Service (South Central – Hampshire A Research Ethics  
573 Committee), Ref 18/SC/0577.

574

575

576 **Author Contributions**

- 577 • Conceived and performed the experiments: AMM, YT, SES, JRB, AK, DQ, CMN, NJE, TAR, FRL, WR,  
578 KJE, J-SC, TDO, AJR, FB, GML, IDP, AM, MZ, MM, RLR, MB, CHM, JCS, NR, CK, NM, CS, TP, KM, DJR,  
579 AMB, PJS, JS, SB, JCR, SJD.
- 580 • Analyzed the data: AMM, YT, SES, JRB, AK, NJE, KJE, J-SC, EA, TDO, AJR, JCS, MMH, BK, JS, SB, JCR,  
581 SJD.
- 582 • Project Management: AML, FLN, KJJ, IJT.
- 583 • Wrote the paper: AMM, AK, SES, JRB, JCR, SJD.

584 **Acknowledgments**

585 This work was funded in part by the European Union's Horizon 2020 research and innovation  
586 programme under grant agreement 733073 for MultiViVax; the UK Medical Research Council (MRC)  
587 Confidence in Concept Scheme at the University of Oxford [MC\_PC\_16056]; and by the National  
588 Institute for Health Research (NIHR) Oxford Biomedical Research Centre (BRC). The views expressed are  
589 those of the authors and not necessarily those of the NIHR or the Department of Health and Social Care.  
590 CMN is a Wellcome Trust Sir Henry Wellcome Postdoctoral Fellow [209200/Z/17/Z]. PJS is the recipient  
591 of a Sir Henry Dale Fellowship jointly funded by the Wellcome Trust and the Royal Society  
592 [107668/Z/15/Z]. TAR held a Wellcome Trust Research Training Fellowship [108734/Z/15/Z]. FB is the  
593 recipient of a Wellcome Trust PhD studentship [203764/Z/16/Z]. AK, EA, TDO, AJR and JCR were  
594 supported by the Wellcome Trust [206194/Z/17/Z]. AMB is supported by the MRC [MR/N00227X/1],  
595 Isaac Newton Trust, Alborada Fund, Wellcome Trust ISSF and University of Cambridge JRG Scheme,  
596 GHIT, Rosetrees Trust and the Royal Society. SB and SJD are Jenner Investigators and SJD held a  
597 Wellcome Trust Senior Fellowship [106917/Z/15/Z].

598

599 The authors are grateful for the assistance of: Julie Furze, Duncan Bellamy, Richard Morter, Catherine  
600 Mair, Lola Matthews, Natalie Lella, Daniel Marshall-Searson, Kathryn Jones and Chris Williams (Jenner  
601 Institute Laboratories and CCVTM, University of Oxford); Richard Tarrant, Eleanor Berrie and Emma  
602 Bolam (Clinical Biomanufacturing Facility, University of Oxford); Julie Staves and the Hematology  
603 Department (Oxford University Hospitals NHS Foundation Trust); Anjali Yadava (WRAIR, USA), Richard  
604 Tedder (Imperial College London, UK) and Nick Day (MORU, Thailand) for clinical advice; Jake Baum  
605 (Imperial College London, UK) for support with mosquito-bite CHMI; Sally Pelling-Deeves and Carly

606 Banner for arranging contracts (University of Oxford); Karl Hoyle for providing training (Applied Science,  
607 UK); Colin Sutherland (LSHTM, UK), Carole Long (NIAID, NIH, USA) and Chetan Chitnis (Pasteur Institute,  
608 France) for providing reagents; members of the Wellcome Sanger Institute DNA Pipelines team,  
609 particularly Mandy Sanders, Craig Corton and Karen Oliver for their advice and input into the DNA  
610 sequencing process; Chris Jacob, Sonia Goncalves and the MalariaGEN team for support with parasite  
611 genotyping; Wai-Hong Tham, Meta Roestenberg and Susan Barnett for providing scientific advice as part  
612 of the MultiViVax Scientific Advisory Board; and all the study volunteers.

613

#### 614 **Conflict of Interest Statement**

615 The authors declare no conflicts of interest.

616

#### 617 **Data and Materials Availability**

618 Requests for materials should be addressed to the corresponding authors.

619

620 The genome assembly and annotation for PvW1 are available from the European Nucleotide Archive  
621 under project accession PRJEB45464.

622

623 **References**

- 624 1. Gething PW, Elyazar IR, Moyes CL, Smith DL, Battle KE, Guerra CA, et al. A long neglected world  
625 malaria map: *Plasmodium vivax* endemicity in 2010. *PLoS Negl Trop Dis*. 2012;6(9):e1814.
- 626 2. Baird JK. Evidence and implications of mortality associated with acute *Plasmodium vivax*  
627 malaria. *Clin Microbiol Rev*. 2013;26(1):36-57.
- 628 3. Galinski MR, and Barnwell JW. *Plasmodium vivax*: who cares? *Malar J*. 2008;7 Suppl 1:S9.
- 629 4. Mueller I, Galinski MR, Baird JK, Carlton JM, Kochar DK, Alonso PL, et al. Key gaps in the  
630 knowledge of *Plasmodium vivax*, a neglected human malaria parasite. *Lancet Infect Dis*.  
631 2009;9(9):555-66.
- 632 5. White NJ. Determinants of relapse periodicity in *Plasmodium vivax* malaria. *Malar J*.  
633 2011;10:297.
- 634 6. Stanisic DI, McCarthy JS, and Good MF. Controlled Human Malaria Infection: Applications,  
635 Advances, and Challenges. *Infect Immun*. 2018;86(1).
- 636 7. Payne RO, Griffin PM, McCarthy JS, and Draper SJ. *Plasmodium vivax* Controlled Human Malaria  
637 Infection - Progress and Prospects. *Trends Parasitol*. 2017;33(2):141-50.
- 638 8. Herrera S, Fernandez O, Manzano MR, Murrain B, Vergara J, Blanco P, et al. Successful  
639 sporozoite challenge model in human volunteers with *Plasmodium vivax* strain derived from  
640 human donors. *Am J Trop Med Hyg*. 2009;81(5):740-6.
- 641 9. Herrera S, Solarte Y, Jordan-Villegas A, Echavarría JF, Rocha L, Palacios R, et al. Consistent safety  
642 and infectivity in sporozoite challenge model of *Plasmodium vivax* in malaria-naïve human  
643 volunteers. *Am J Trop Med Hyg*. 2011;84(2 Suppl):4-11.
- 644 10. Arevalo-Herrera M, Forero-Pena DA, Rubiano K, Gomez-Hincapie J, Martinez NL, Lopez-Perez M,  
645 et al. *Plasmodium vivax* sporozoite challenge in malaria-naïve and semi-immune Colombian  
646 volunteers. *PLoS One*. 2014;9(6):e99754.
- 647 11. Arevalo-Herrera M, Vasquez-Jimenez JM, Lopez-Perez M, Vallejo AF, Amado-Garavito AB,  
648 Cespedes N, et al. Protective Efficacy of *Plasmodium vivax* Radiation-Attenuated Sporozoites in  
649 Colombian Volunteers: A Randomized Controlled Trial. *PLoS Negl Trop Dis*.  
650 2016;10(10):e0005070.
- 651 12. Bennett JW, Yadava A, Tosh D, Sattabongkot J, Komisar J, Ware LA, et al. Phase 1/2a Trial of  
652 *Plasmodium vivax* Malaria Vaccine Candidate VMP001/AS01B in Malaria-Naïve Adults: Safety,  
653 Immunogenicity, and Efficacy. *PLoS Negl Trop Dis*. 2016;10(2):e0004423.
- 654 13. Bennett JW, Pybus BS, Yadava A, Tosh D, Sousa JC, McCarthy WF, et al. Primaquine Failure and  
655 Cytochrome P-450 2D6 in *Plasmodium vivax* Malaria. *N Engl J Med*. 2013;369(14):1381-2.
- 656 14. Duncan CJ, and Draper SJ. Controlled human blood stage malaria infection: current status and  
657 potential applications. *Am J Trop Med Hyg*. 2012;86(4):561-5.
- 658 15. Engwerda CR, Minigo G, Amante FH, and McCarthy JS. Experimentally induced blood stage  
659 malaria infection as a tool for clinical research. *Trends Parasitol*. 2012;28(11):515-21.
- 660 16. Payne RO, Milne KH, Elias SC, Edwards NJ, Douglas AD, Brown RE, et al. Demonstration of the  
661 Blood-Stage Controlled Human Malaria Infection Model to Assess Efficacy of the *Plasmodium*  
662 *falciparum* AMA1 Vaccine FMP2.1/AS01. *J Infect Dis*. 2016;213(11):1743-51.
- 663 17. Alkema M, Reuling IJ, de Jong GM, Lanke K, Coffeng LE, van Gemert GJ, et al. A randomized  
664 clinical trial to compare *P. falciparum* gametocytaemia and infectivity following blood-stage or  
665 mosquito bite induced controlled malaria infection. *J Infect Dis*. 2020.
- 666 18. Milne K, Ivens A, Reid AJ, Lotkowska ME, O'Toole A, Sankaranarayanan G, et al. Mapping  
667 immune variation and var gene switching in naïve hosts infected with *Plasmodium falciparum*.  
668 *eLife*. 2021;10.

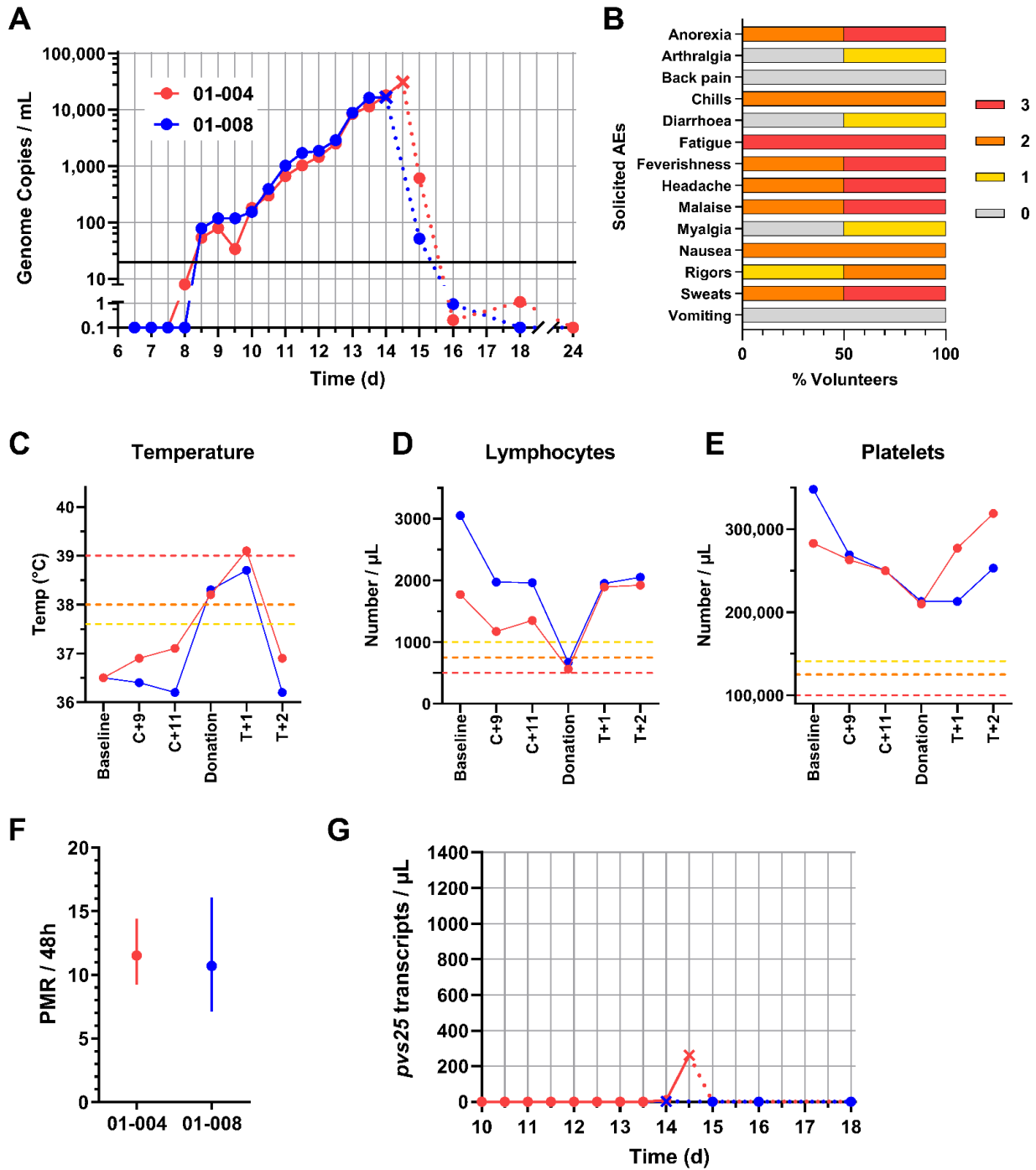
- 669 19. McCarthy JS, Griffin PM, Sekuloski S, Bright AT, Rockett R, Looke D, et al. Experimentally induced  
670 blood-stage *Plasmodium vivax* infection in healthy volunteers. *J Infect Dis.* 2013;208(10):1688-  
671 94.
- 672 20. Griffin P, Pasay C, Elliott S, Sekuloski S, Sikulu M, Hugo L, et al. Safety and Reproducibility of a  
673 Clinical Trial System Using Induced Blood Stage *Plasmodium vivax* Infection and Its Potential as a  
674 Model to Evaluate Malaria Transmission. *PLoS Negl Trop Dis.* 2016;10(12):e0005139.
- 675 21. Collins KA, Wang CY, Adams M, Mitchell H, Rampton M, Elliott S, et al. A controlled human  
676 malaria infection model enabling evaluation of transmission-blocking interventions. *J Clin Invest.*  
677 2018;128(4):1551-62.
- 678 22. Collins KA, Abd-Rahman AN, Marquart L, Ballard E, Gobeau N, Griffin P, et al. Antimalarial  
679 activity of artefenomel against asexual parasites and transmissible gametocytes during  
680 experimental blood-stage *Plasmodium vivax* infection. *J Infect Dis.* 2020.
- 681 23. Odedra A, Mudie K, Kennedy G, Watts RE, Rossignol E, Mitchell H, et al. Safety and feasibility of  
682 apheresis to harvest and concentrate parasites from subjects with induced blood stage  
683 *Plasmodium vivax* infection. *Malar J.* 2021;20(1):43.
- 684 24. Spence PJ, Jarra W, Levy P, Reid AJ, Chappell L, Brugat T, et al. Vector transmission regulates  
685 immune control of *Plasmodium* virulence. *Nature.* 2013;498(7453):228-31.
- 686 25. Miller LH, Mason SJ, Clyde DF, and McGinniss MH. The resistance factor to *Plasmodium vivax* in  
687 blacks. The Duffy-blood-group genotype, FyFy. *N Engl J Med.* 1976;295(6):302-4.
- 688 26. Baird JK. 8-Aminoquinoline Therapy for Latent Malaria. *Clin Microbiol Rev.* 2019;32(4).
- 689 27. Rebsamen MC, Desmeules J, Daali Y, Chiappe A, Diemand A, Rey C, et al. The AmpliChip CYP450  
690 test: cytochrome P450 2D6 genotype assessment and phenotype prediction. *Pharmacogenomics*  
691 *J.* 2009;9(1):34-41.
- 692 28. Douglas AD, Edwards NJ, Duncan CJ, Thompson FM, Sheehy SH, O'Hara GA, et al. Comparison of  
693 Modeling Methods to Determine Liver-to-blood Inocula and Parasite Multiplication Rates During  
694 Controlled Human Malaria Infection. *J Infect Dis.* 2013;208(2):340-5.
- 695 29. Payne RO, Silk SE, Elias SC, Milne KH, Rawlinson TA, Llewellyn D, et al. Human vaccination  
696 against *Plasmodium vivax* Duffy-binding protein induces strain-transcending antibodies. *JCI*  
697 *Insight.* 2017;2(12):93683.
- 698 30. Auburn S, Bohme U, Steinbiss S, Trimarsanto H, Hostetler J, Sanders M, et al. A new *Plasmodium*  
699 *vivax* reference sequence with improved assembly of the subtelomeres reveals an abundance of  
700 *pir* genes. *Wellcome open research.* 2016;1:4.
- 701 31. Carlton JM, Adams JH, Silva JC, Bidwell SL, Lorenzi H, Caler E, et al. Comparative genomics of the  
702 neglected human malaria parasite *Plasmodium vivax*. *Nature.* 2008;455(7214):757-63.
- 703 32. Lopez FJ, Bernabeu M, Fernandez-Becerra C, and del Portillo HA. A new computational approach  
704 redefines the subtelomeric *vir* superfamily of *Plasmodium vivax*. *BMC Genomics.* 2013;14:8.
- 705 33. Rice BL, Acosta MM, Pacheco MA, Carlton JM, Barnwell JW, and Escalante AA. The origin and  
706 diversification of the merozoite surface protein 3 (*m*sp3) multi-gene family in *Plasmodium vivax*  
707 and related parasites. *Mol Phylogenet Evol.* 2014;78:172-84.
- 708 34. Draper SJ, Sack BK, King CR, Nielsen CM, Rayner JC, Higgins MK, et al. Malaria Vaccines: Recent  
709 Advances and New Horizons. *Cell Host Microbe.* 2018;24(1):43-56.
- 710 35. Arnot DE, Barnwell JW, Tam JP, Nussenzweig V, Nussenzweig RS, and Enea V. Circumsporozoite  
711 protein of *Plasmodium vivax*: gene cloning and characterization of the immunodominant  
712 epitope. *Science.* 1985;230(4727):815-8.
- 713 36. Rosenberg R, Wirtz RA, Lanar DE, Sattabongkot J, Hall T, Waters AP, et al. Circumsporozoite  
714 protein heterogeneity in the human malaria parasite *Plasmodium vivax*. *Science.*  
715 1989;245(4921):973-6.

- 716 37. Singh K, Mukherjee P, Shakri AR, Singh A, Pandey G, Bakshi M, et al. Malaria vaccine candidate  
717 based on Duffy-binding protein elicits strain transcending functional antibodies in a Phase I trial.  
718 *NPJ Vaccines*. 2018;3:48.
- 719 38. Chen E, Salinas ND, Ntumngia FB, Adams JH, and Tolia NH. Structural Analysis of the Synthetic  
720 Duffy Binding Protein (DBP) Antigen DEKnull Relevant for Plasmodium vivax Malaria Vaccine  
721 Design. *PLoS Negl Trop Dis*. 2015;9(3):e0003644.
- 722 39. Menard D, Chan ER, Benedet C, Ratsimbaoa A, Kim S, Chim P, et al. Whole genome sequencing  
723 of field isolates reveals a common duplication of the Duffy binding protein gene in Malagasy  
724 Plasmodium vivax strains. *PLoS Negl Trop Dis*. 2013;7(11):e2489.
- 725 40. Hostetler JB, Lo E, Kanjee U, Amaratunga C, Suon S, Sreng S, et al. Independent Origin and  
726 Global Distribution of Distinct Plasmodium vivax Duffy Binding Protein Gene Duplications. *PLoS*  
727 *Negl Trop Dis*. 2016;10(10):e0005091.
- 728 41. Popovici J, Roesch C, Carias LL, Khim N, Kim S, Vantaux A, et al. Amplification of Duffy binding  
729 protein-encoding gene allows Plasmodium vivax to evade host anti-DBP humoral immunity. *Nat*  
730 *Commun*. 2020;11(1):953.
- 731 42. Pearson RD, Amato R, Auburn S, Miotto O, Almagro-Garcia J, Amaratunga C, et al. Genomic  
732 analysis of local variation and recent evolution in Plasmodium vivax. *Nat Genet*. 2016;48(8):959-  
733 64.
- 734 43. Auliff AM, Adams JH, O'Neil MT, and Cheng Q. Defining the role of mutations in Plasmodium  
735 vivax dihydrofolate reductase-thymidylate synthase gene using an episomal Plasmodium  
736 falciparum transfection system. *Antimicrob Agents Chemother*. 2010;54(9):3927-32.
- 737 44. Pornthanakasem W, Riengrunroj P, Chitnumsub P, Ittarat W, Kongkasuriyachai D, Uthaipibull C,  
738 et al. Role of Plasmodium vivax Dihydropteroate Synthase Polymorphisms in Sulfa Drug  
739 Resistance. *Antimicrob Agents Chemother*. 2016;60(8):4453-63.
- 740 45. Suwanarusk R, Russell B, Chavchich M, Chalfein F, Kenangalem E, Kosaisavee V, et al.  
741 Chloroquine resistant Plasmodium vivax: in vitro characterisation and association with  
742 molecular polymorphisms. *PLoS One*. 2007;2(10):e1089.
- 743 46. Suwanarusk R, Chavchich M, Russell B, Jaidee A, Chalfein F, Barends M, et al. Amplification of  
744 pvmdr1 associated with multidrug-resistant Plasmodium vivax. *J Infect Dis*. 2008;198(10):1558-  
745 64.
- 746 47. Lu F, Lim CS, Nam DH, Kim K, Lin K, Kim TS, et al. Genetic polymorphism in pvmdr1 and pvcrt-o  
747 genes in relation to in vitro drug susceptibility of Plasmodium vivax isolates from malaria-  
748 endemic countries. *Acta Trop*. 2011;117(2):69-75.
- 749 48. Chen N, Auliff A, Rieckmann K, Gatton M, and Cheng Q. Relapses of Plasmodium vivax infection  
750 result from clonal hypnozoites activated at predetermined intervals. *J Infect Dis*.  
751 2007;195(7):934-41.
- 752 49. Imwong M, Snounou G, Pukrittayakamee S, Tanomsing N, Kim JR, Nandy A, et al. Relapses of  
753 Plasmodium vivax infection usually result from activation of heterologous hypnozoites. *J Infect*  
754 *Dis*. 2007;195(7):927-33.
- 755 50. Bright AT, Manary MJ, Tewhey R, Arango EM, Wang T, Schork NJ, et al. A high resolution case  
756 study of a patient with recurrent Plasmodium vivax infections shows that relapses were caused  
757 by meiotic siblings. *PLoS Negl Trop Dis*. 2014;8(6):e2882.
- 758 51. Mikolajczak SA, Vaughan AM, Kangwanransan N, Roobsoong W, Fishbaugher M,  
759 Yimamnuaychok N, et al. Plasmodium vivax liver stage development and hypnozoite persistence  
760 in human liver-chimeric mice. *Cell Host Microbe*. 2015;17(4):526-35.
- 761 52. Malaria parasite strain characterization, cryopreservation, and banking of isolates: a WHO  
762 memorandum. *Bull World Health Organ*. 1981;59(4):537-48.

- 763 53. Minassian AM, Silk SE, Barrett JR, Nielsen CM, Miura K, Diouf A, et al. Reduced blood-stage  
764 malaria growth and immune correlates in humans following RH5 vaccination. *Med.* 2021;2:1-19.
- 765 54. Kamau E, Bennett JW, and Yadava A. Safety and Tolerability of Mosquito-Bite Induced  
766 Controlled Human Infection with *P. vivax* in Malaria-Naive Study Participants - Clinical Profile  
767 and Utility of Molecular Diagnostic Methods. *J Infect Dis.* 2021.
- 768 55. Odedra A, Webb L, Marquart L, Britton LJ, Chalon S, Moehrle JJ, et al. Liver Function Test  
769 Abnormalities in Experimental and Clinical *Plasmodium vivax* Infection. *Am J Trop Med Hyg.*  
770 2020;103(5):1910-7.
- 771 56. Arevalo-Herrera M, Lopez-Perez M, Dotsey E, Jain A, Rubiano K, Felgner PL, et al. Antibody  
772 Profiling in Naive and Semi-immune Individuals Experimentally Challenged with *Plasmodium*  
773 *vivax* Sporozoites. *PLoS Negl Trop Dis.* 2016;10(3):e0004563.
- 774 57. Biswas S, Choudhary P, Elias SC, Miura K, Milne KH, de Cassan SC, et al. Assessment of Humoral  
775 Immune Responses to Blood-Stage Malaria Antigens following ChAd63-MVA Immunization,  
776 Controlled Human Malaria Infection and Natural Exposure. *PLoS One.* 2014;9(9):e107903.
- 777 58. Hodgson SH, Llewellyn D, Silk SE, Milne KH, Elias SC, Miura K, et al. Changes in Serological  
778 Immunology Measures in UK and Kenyan Adults Post-controlled Human Malaria Infection. *Front*  
779 *Microbiol.* 2016;7:1604.
- 780 59. Mohring F, Hart MN, Rawlinson TA, Henrici R, Charleston JA, Diez Benavente E, et al. Rapid and  
781 iterative genome editing in the malaria parasite *Plasmodium knowlesi* provides new tools for *P.*  
782 *vivax* research. *eLife.* 2019;8.
- 783 60. King CL, Adams JH, Xianli J, Grimberg BT, McHenry AM, Greenberg LJ, et al. Fy(a)/Fy(b) antigen  
784 polymorphism in human erythrocyte Duffy antigen affects susceptibility to *Plasmodium vivax*  
785 malaria. *Proc Natl Acad Sci U S A.* 2011;108(50):20113-8.
- 786 61. Vallejo AF, Garcia J, Amado-Garavito AB, Arevalo-Herrera M, and Herrera S. *Plasmodium vivax*  
787 gametocyte infectivity in sub-microscopic infections. *Malar J.* 2016;15:48.
- 788 62. Kingan SB, Heaton H, Cudini J, Lambert CC, Baybayan P, Galvin BD, et al. A High-Quality De novo  
789 Genome Assembly from a Single Mosquito Using PacBio Sequencing. *Genes (Basel).* 2019;10(1).
- 790 63. Harrison TE, Morch AM, Felce JH, Sakoguchi A, Reid AJ, Arase H, et al. Structural basis for RIFIN-  
791 mediated activation of LILRB1 in malaria. *Nature.* 2020;587(7833):309-12.
- 792 64. Bach F, Sandoval DM, Mazurczyk M, Themistocleous Y, Rawlinson TA, Kemp A, et al. Parasite  
793 species regulates T cell activation in human malaria. *medRxiv.* 2021:2021.03.22.21252810.
- 794 65. Hodgson SH, Juma E, Salim A, Magiri C, Kimani D, Njenga D, et al. Evaluating controlled human  
795 malaria infection in Kenyan adults with varying degrees of prior exposure to *Plasmodium*  
796 *falciparum* using sporozoites administered by intramuscular injection. *Front Microbiol.*  
797 2014;5:686.

798

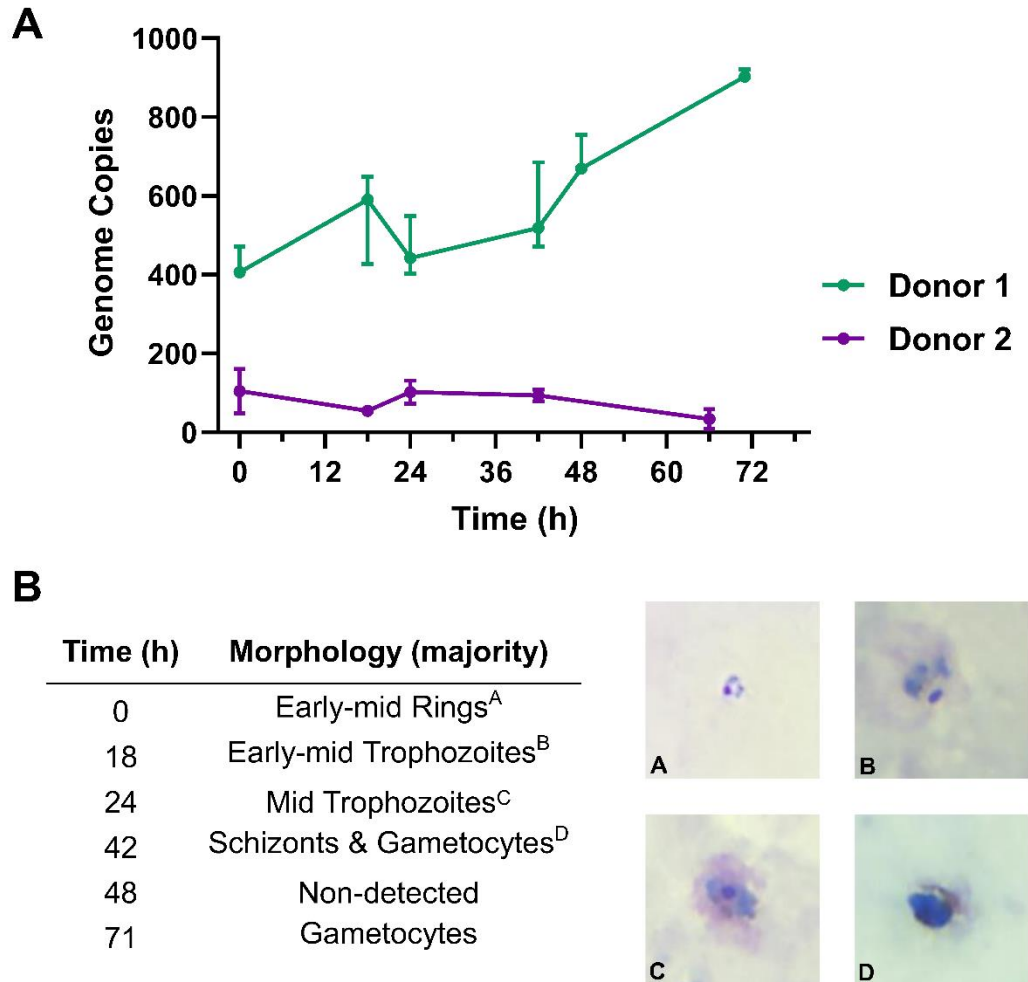
799 **Figures and Legends**



800  
 801 **Figure 1. Safety and parasite growth dynamics of *P. vivax* sporozoite CHMI.**  
 802 (A) qPCR data for the VAC068 trial (n=2). Parasitemia measured in genome copies / mL is shown over  
 803 time for each volunteer. CHMI was initiated by mosquito bite on day 0. Cross symbols indicate the time-  
 804 point of blood donation followed by anti-malarial treatment. Solid lines show qPCR readouts pre-

805 treatment, and dotted lines post-treatment. Solid black line indicates 20 gc/mL (the minimum level to  
806 meet positive reporting criteria); samples below this are shown for information only. **(B)** The solicited  
807 systemic adverse events (AEs) recorded during the CHMI period (from 1 day up until 45 days post-  
808 challenge) are shown as the maximum severity reported by each volunteer and as a percentage of the  
809 volunteers reporting each individual AE (n=2). Color-coding refers to AE grading: 0 = none; 1 = mild; 2 =  
810 moderate; 3 = severe. **(C)** Volunteer temperature (maximum self-recorded by volunteer or measured in  
811 clinic) at the indicated time-points: baseline pre-CHMI; 9 and 11 days post-CHMI (C+9, C+11); time of  
812 blood donation; and 1 and 2 days post-treatment (T+1, T+2). AE grading cut-offs are indicated by the  
813 dotted lines (yellow = grade 1; orange = grade 2; red = grade 3). **(D)** Lymphocyte and **(E)** platelet counts  
814 plotted as for panel C. **(F)** The PMR per 48 h was modelled from the qPCR data up until the time-point of  
815 blood donation/treatment; PMR  $\pm$  95% CI is shown for each volunteer. **(H)** Gametocytemia was assessed  
816 over time by qRT-PCR for *pvs25* transcripts; symbols and lines as per panel A.

817

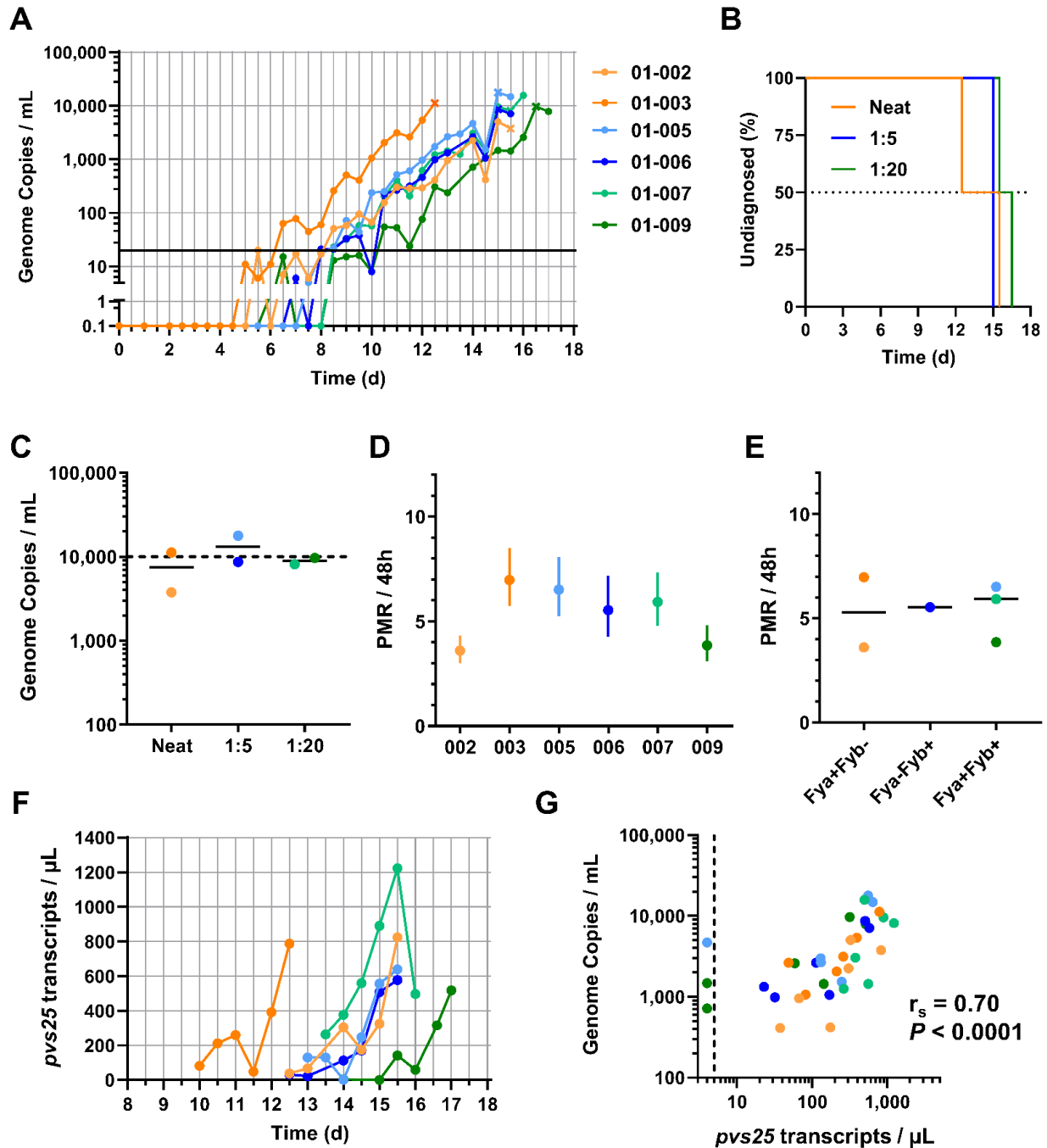


818

819 **Figure 2. Test of cryopreserved parasite viability by short-term *in vitro* culture assay.**

820 (A) Test vials of cryopreserved parasites from Donor 1 and Donor 2 were thawed and cells used in a  
 821 short-term *in vitro* parasite culture assay. *P. vivax* parasite growth was monitored by qPCR in 20  $\mu$ L  
 822 samples of RBC extracted at the indicated time-points. Median and range of triplicate readings are  
 823 shown in genome copies measured per 20  $\mu$ L sample. (B) Parasite morphology was monitored at the  
 824 same time-points over the first growth cycle by light microscopy of Giemsa-stained thick and thin blood  
 825 films Representative images are shown from Donor 1, and the predominant morphology observed is  
 826 reported.

827



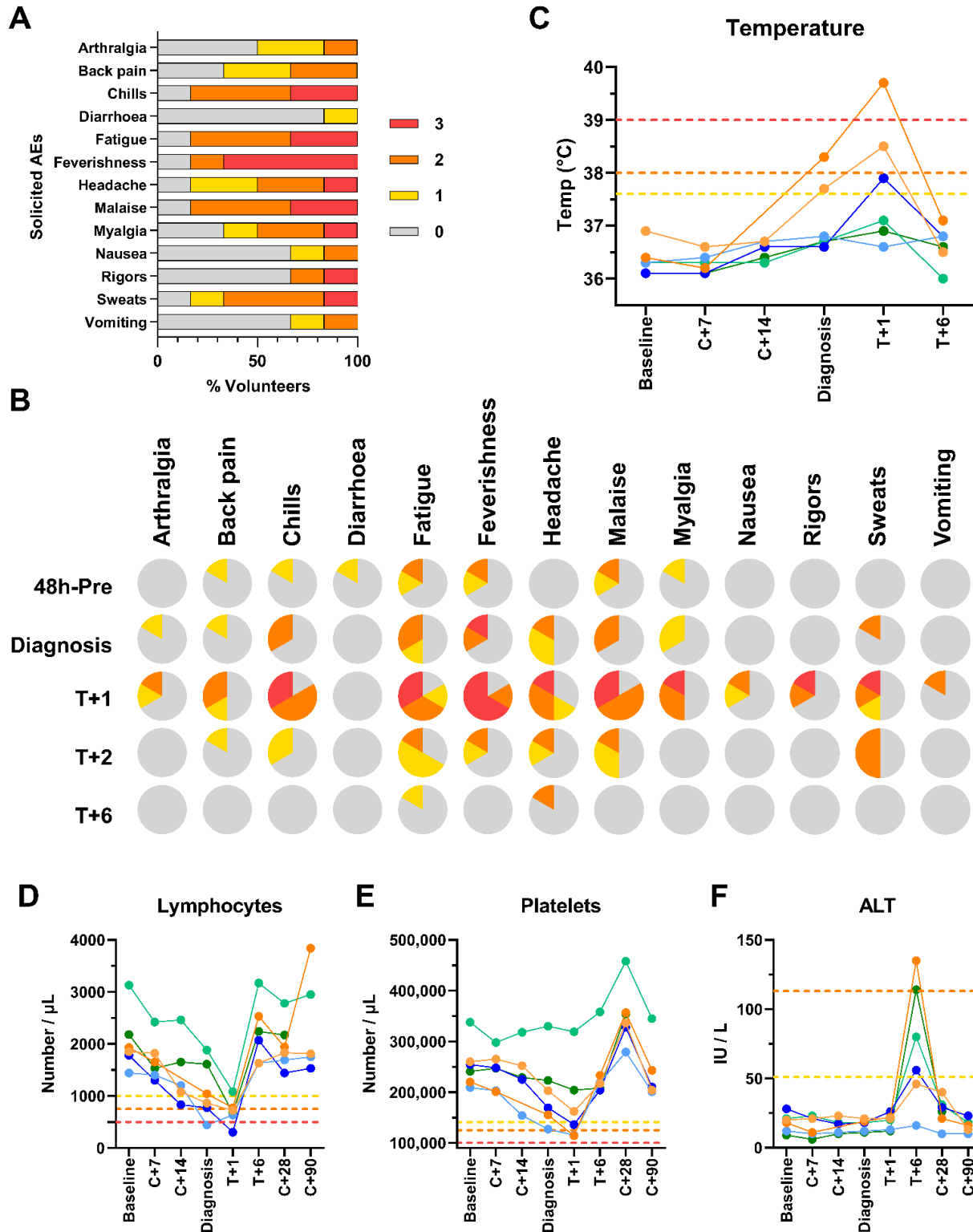
828

829 **Figure 3. Parasite growth dynamics of *P. vivax* PvW1 clone blood-stage CHMI.**

830 (A) qPCR data for the VAC069A trial (n=6). Parasitemia measured in genome copies (gc) / mL is shown  
 831 over time for each volunteer. CHMI was initiated by blood-stage inoculation on day 0. Cross symbols  
 832 indicate the time-point of diagnosis. Orange = neat inoculum dose; blue = 1:5 and green = 1:20 dilution  
 833 of the neat inoculum dose. Solid black line indicates 20 gc/mL (the minimum level to meet positive  
 834 reporting criteria); samples below this are shown for information only. (B) Kaplan-Meier plot of time to

835 diagnosis in days for the VAC069A study (n=2/group). **(C)** Parasitemia measured in gc/mL at the time-  
836 point of diagnosis. Individual data and median are indicated for each dose group. Volunteers were  
837 diagnosed when they reached a threshold of 10,000 gc/mL OR if they had symptoms of malaria with a  
838 parasitemia >5,000 gc/mL. **(D)** The PMR per 48 h was modelled from the qPCR data up until the time-  
839 point of diagnosis; PMR  $\pm$  95% CI is shown for each volunteer. **(E)** Individual and median PMR are shown  
840 with volunteers grouped according to their Duffy blood group antigen (Fy) serological phenotype. **(F)**  
841 Gametocytemia was assessed over time by qRT-PCR for *pvs25* transcripts; colored lines as per panel A.  
842 **(G)** Correlation of total parasitemia measured in gc/mL versus *pvs25* transcripts/ $\mu$ L. Spearman's rank  
843 correlation coefficient and *P* value are shown, n=36.

844



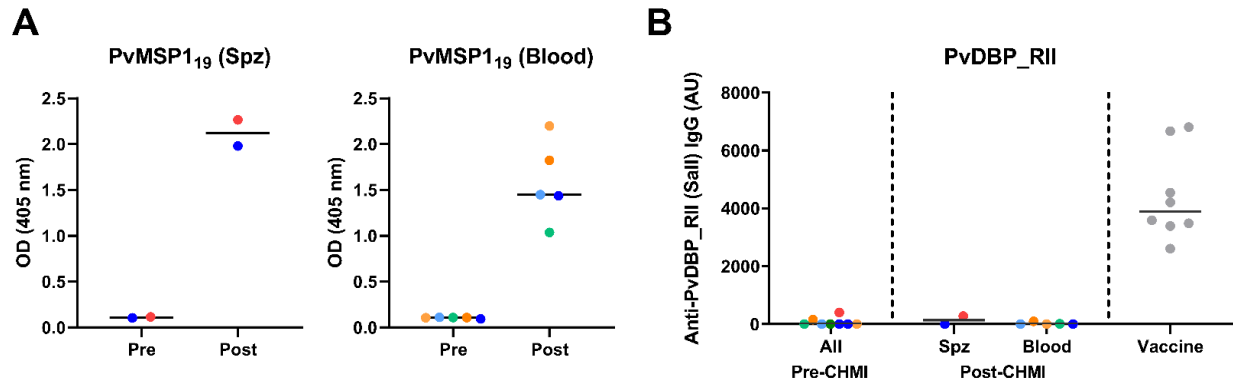
845

846 **Figure 4. Safety analysis of *P. vivax* PvW1 clone blood-stage CHMI.**

847 **(A)** The solicited systemic adverse events (AEs) recorded during the CHMI period (from 1 day up until 90  
 848 days post-challenge) are shown as the maximum severity reported by each volunteer and as a

849 percentage of the volunteers reporting each individual AE (n=6). Color-coding refers to AE grading: 0 =  
850 none; 1 = mild; 2 = moderate; 3 = severe. **(B)** The solicited systemic AEs recorded at the indicated time-  
851 points during the CHMI period are shown as the maximum severity reported by each volunteer and as a  
852 percentage of the volunteers reporting each individual AE (n=6). Color-coding as per panel A. 48h-pre =  
853 the 48 hour period prior to *P. vivax* diagnosis; Diagnosis = time-point of diagnosis; +1, +2 and +6 days  
854 post-treatment (T). **(C)** Volunteer temperature (maximum self-recorded by volunteer or measured in  
855 clinic) at the indicated time-points: baseline pre-CHMI; 7 and 14 days post-CHMI (C+7, C+14); time of  
856 diagnosis; and 1 and 6 days post-treatment (T+1, T+6). AE grading cut-offs are indicated by the dotted  
857 lines (yellow = grade 1; orange = grade 2; red = grade 3). **(D)** Lymphocyte and **(E)** platelet counts, and **(F)**  
858 alanine aminotransferase (ALT) measurements, all plotted as for panel C but also including C+28 and  
859 C+90 time-points.

860

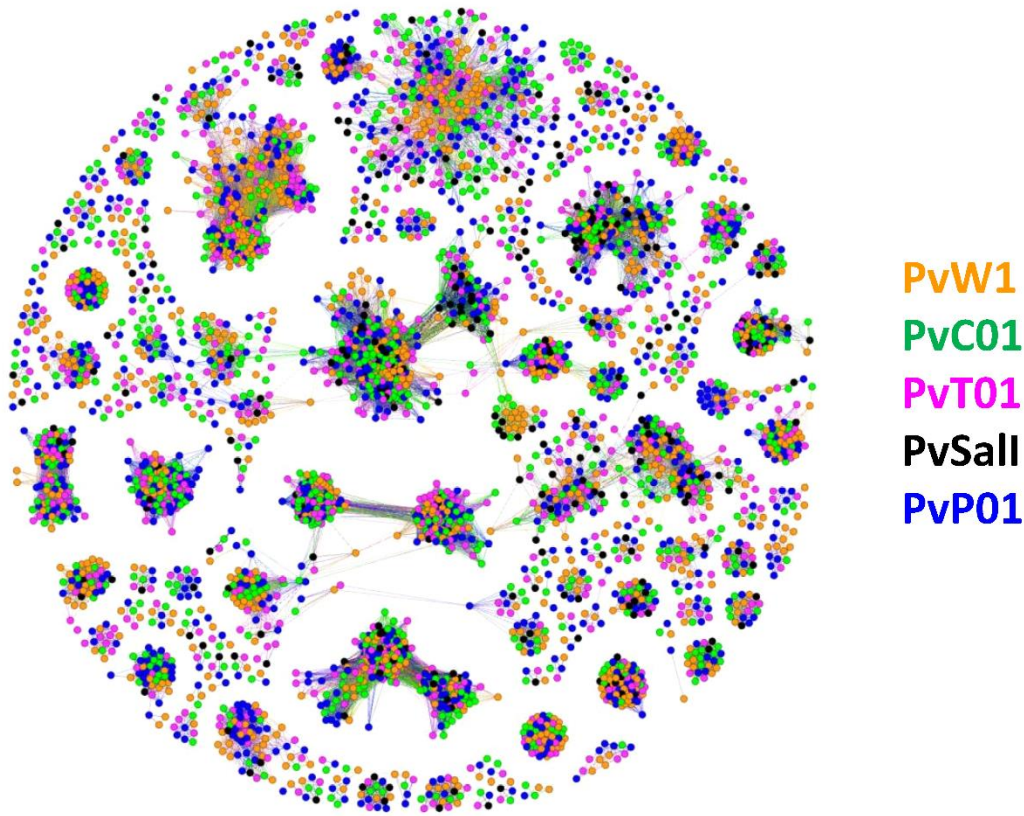


861

862 **Figure 5. Induction of serum antibody responses to merozoite antigens during CHMI.**

863 **(A)** Serum anti-PvMSP1<sub>19</sub> IgG ELISA was conducted on samples from the VAC068 mosquito-bite /  
 864 sporozoite (spz) CHMI study (n=2) and the VAC069A blood-stage CHMI study (n=5, because one  
 865 volunteer withdrew at dC+28). Optical density (OD) 405nm data are shown for sera tested at a 1:100  
 866 dilution from the pre-CHMI (dC-1) and 90 days post-CHMI (dC+90) time-points. Samples color-coded as  
 867 per previous figures. **(B)** Serum anti-PvDBP\_RII (Sall allele) IgG as measured by standardized ELISA,  
 868 reporting in arbitrary units (AU). Same samples tested as in panel A. Vaccine = positive control samples  
 869 (n=8) from a previous Phase Ia clinical trial of a PvDBP\_RII vaccine (29). Individual data and median are  
 870 shown.

871



872

873 **Figure 6. Cluster analysis of the PvW1 vivax interspersed repeat (VIR) proteins.**

874 Cluster analysis of the 1145 predicted VIR proteins encoded by the PvW1 genome compared to those of  
875 other *P. vivax* isolates (30, 31). Each spot represents a VIR protein from either PvW1 (orange), PvC01  
876 (green), PvT01 (pink), PvSall (black) and PvP01 (blue). Relatedness between the proteins is represented  
877 by distance, therefore more closely related proteins cluster together. Most of the clusters contain  
878 proteins from several isolates suggesting that the clusters are not restricted to specific genomes or  
879 geographical distribution.

880 **Table**

881

| Genome Features                  | PvW1 | PvP01 | PvC01 | PvT01 | Sall |
|----------------------------------|------|-------|-------|-------|------|
| <b>Nuclear genome</b>            |      |       |       |       |      |
| Assembly size (Mb)               | 28.9 | 29    | 30.2  | 28.9  | 26.8 |
| G + C content (%)                | 39.9 | 39.8  | 39.2  | 39.7  | 42.3 |
| No. scaffolds assigned to chrom. | 14   | 14    | 14    | 14    | 30   |
| No. unassigned scaffolds         | 3    | 226   | 529   | 359   | 2745 |
| No. genes                        | 6583 | 6642  | 6690  | 6464  | 5433 |
| No. pir (VIR) genes              | 1145 | 1212  | 1061  | 867   | 346  |
| <b>Mitochondrial genome</b>      |      |       |       |       |      |
| Assembly size (bp)               | 5994 | 5989  | -     | -     | 5990 |
| G + C content (%)                | 30.5 | 30.5  | -     | -     | 30.5 |
| <b>Apicoplast genome</b>         |      |       |       |       |      |
| Assembly size (kb)               | 34.5 | 29.6  | 27.6  | 6.6   | 5.1  |
| G + C content (%)                | 14.4 | 13.3  | 12.7  | 19.7  | 17.1 |
| No. genes                        | 54   | 30    | 3     | 0     | 0    |

882

883 **Table 1. Comparison of genome assembly statistics between PvW1 and other *P. vivax***  
884 **assemblies.**

885 PvW1 genome assembly statistics were compared with the best available existing assemblies: PvP01,

886 PvC01, PvT01 and Sall (30, 31). pir = *P. vivax Plasmodium* interspersed repeat, also known as VIR.